Infectious Disease Modelling 6 (2021) 782–804

Contents lists available at ScienceDirect

Infectious Disease Modelling

journal homepage: www.keaipublishing.com/idm

Analysis and optimal control of a Huanglongbing mathematical model with resistant vector

Youquan Luo [a, **], Fumin Zhang [a], Yujiang Liu [a], Shujing Gao [a, b, *]

[a] Key Laboratory of Jiangxi Province for Numerical Simulation and Emulation Techniques, Gannan Normal University, Ganzhou, 341000, PR China

[b] National Navel Orange Engineering Research Center, Gannan Normal University, Ganzhou, 341000, PR China

ARTICLE INFO

Article history:
Received 21 April 2021
Received in revised form 24 May 2021
Accepted 28 May 2021
Available online 6 June 2021
Handling editor: Dr Lou Yijun

Keywords:
Huanglongbing
Insecticide resistance
Dynamic model
Optimal control
Sensitivity analysis

ABSTRACT

Huanglongbing (HLB) is an incurable disease that affects citrus trees. To better understand the transmission of HLB, the mathematical model is developed to investigate the transmission dynamics of the disease between Asian citrus psyllid (ACP) and citrus trees. Through rigorous mathematical derivations, we derive the expression of the basic reproduction number (R_0) of HLB. The findings show that the disease-free equilibrium is locally asymptotically stable if $R_0 < 1$, and if $R_0 > 1$ the system is uniformly persistent. By applying the global sensitivity analysis of R_0, we can obtain some parameters that have the greatest influence on the HLB transmission dynamics. Additionally, the optimal control theory is used to explore the corresponding optimal control problem of the HLB model. Numerical simulations are conducted to reinforce the analytical results. These theoretical and numerical results provide useful insights for understanding the transmission dynamics of HLB and may help policy makers to develop intervention strategies for the disease.

1. Introduction

Huanglongbing (HLB) is one of the most destructive diseases of citrus, which is caused by the bacterium Candidatus Liberibacter asiaticus (CLas) and vectored by the Asian citrus psyllid (ACP) (Bovè, 2006; Gottwald, 2010; Li et al., 2015). It is regarded as the most devastating citrus disease worldwide, and was first found in southern China in 1919, and now it is transmitted in fifty different countries (Bovè, 2006; Wang & Trivedi, 2013). It causes substantial economic burdens to individual growers, citrus industries and governments (Taylor et al., 2016). Recently, citrus production has endured serious economic losses due to the occurrence of citrus HLB disease. This disease reduces fruit quality and yield, infringes on citrus health and has become one of the biggest challenges for citrus growers all over the world (Arredondo Valdés et al., 2016). The United States, Brazil and China, the world's largest citrus producers, are all threatened by HLB disease. Up to now, there is still no effective method to eradicate HLB, and once orchards are infected with the disease, they are often destroyed due to low yields (McCollum & Baldwin, 2017). In view of

* Corresponding author. Key Laboratory of Jiangxi Province for Numerical Simulation and Emulation Techniques, Gannan Normal University, Ganzhou, 341000, PR China.
** Corresponding author.
E-mail addresses: lyq637485@163.com (Y. Luo), gaosjmath@126.com (S. Gao).
Peer review under responsibility of KeAi Communications Co., Ltd.

https://doi.org/10.1016/j.idm.2021.05.004

the serious impact of HLB on the agricultural economy, it is of great importance to understand HLB transmission dynamics between citrus trees and ACP and to implement some effective intervention strategies to curb its transmission (Chiyaka et al., 2012).

Mathematical models have been playing a vital role in understanding HLB disease transmission dynamics and also in decision making processes regarding intervention mechanisms for the disease control (Chowdhury et al., 2019; Jackson & Chen-Charpentier, 2019; Jeger et al., 2018; Li et al., 2020; Meng & Li, 2010; Zhang et al., 2021; Zhang & Georgescu, 2015; Zhao et al., 2017). However, despite their significant impact on the agricultural economy, very few mathematical models have investigated how HLB disease is transmitted between the insect vector and the host (Taylor et al., 2016; Chiyaka et al., 2012; Lee et al., 2015; Vilamiu et al., 1479; Jacobsen et al., 2013; Gao et al., 2018; Khan et al., 2021). For the goal of highlighting the importance of flush for ACP dynamics, Chiyaka and Halbert (Chiyaka et al., 2012) formulated a mathematical model to study the spread of HLB within a tree because the infection payllid transmits among the different flush patches on the tree. To explore the impact of seasonal fluctuations on HLB disease, Gao and Yu (Gao et al., 2018) built an impulsive switching model for the disease with seasonal fluctuations. Jacobsen and Stupiansky (Jacobsen et al., 2013) investigated a deterministic model for HLB transmission within a single citrus garden, which included the intervention strategy of roguing. Other further studies include Tu and Gao (Tu et al., 2019) developed a vector-borne disease model with stage structure and analyzed the effect of the measure in controlling the spread of HLB. We review those models that have been applied to HLB here because they show the main insights models have provided for this disease system.

Although some of the studies mentioned above took into account different mathematical models of HLB and disease intervention strategies, they did not consider the optimality of these intervention strategies and the resistance of the vector ACP, which may sometimes be limited by resource availability. In particular, a comparative analysis to understand the costs of different intervention strategies is important for decision makers who are often faced with the resource allocation challenges. In view of this, the application of optimal control theory can serve as a useful tool for assessing the effectiveness of various policies and interventions relative to the cost of implementing them (Alzahrani et al., 2021; Khan & Fatmawatic, 2021; Okosun et al., 2013). Based on these considerations, in this paper, we formulate a compartmental model to investigate HLB transmission dynamics with resistant ACP in a single orchard of citrus trees. Through extensive calculations, we obtain the basic reproduction number, i.e., the HLB disease below this threshold disappears but outbreaks above this threshold. The persistence of the system is further explored. Subsequently, optimal control theory is used to study the effectiveness and optimality of all possible combinations of two interventions for HLB disease, i.e., removing trees with HLB symptoms and spraying insecticides. We derive the optimal control conditions by using the Pontryagin s Maximum Principle (Pontryagin, 2018). Furthermore, we obtain through numerical experiments that the optimal control strategy outperforms the constant intervention strategy in reducing the prevalence of the diseased citrus trees, and the cost of implementing the optimal control is far lower than the constant intervention strategy.

The remaining of this paper is organized as follows: the deterministic mathematical model is proposed to study the HLB transmission dynamics which incorporates ACP and citrus trees in Section 2. The basic reproduction number and local stability of the eight-dimensional HLB system are obtained in Section 3. Furthermore, the uniformly persistent of the nonlinear system are explored. The optimal control problem of the compartment model is conducted in Section 4. The global sensitivity and uncertainty analysis are performed, and some suggestions for HLB intervention strategies from the proposed model are summarized in Section 5. Finally, this paper ends with a brief conclusion and the potential outlook for future work in Section 6.

2. Model formulation

According to the work of (Hu et al., 2018), it was reported that trunk injection of penicillin, streptomycin and oxytetracycline hydrochloride, were effective in reducing the concentration of CLas and slowing down progress of HLB disease. In this paper, the model analyses the transmission dynamics of HLB with fraction of susceptible vaccinated citrus tress. Therefore, the citrus tree population given as $N_h(t)$ is divided into susceptible individuals ($S_h(t)$), vaccinated individuals ($V_h(t)$), exposed individuals ($E_h(t)$), and infected individuals ($I_h(t)$), at any time t. Thus, $N_h(t) = S_h(t) + V_h(t) + E_h(t) + I_h(t)$. The ACP population, denoted by $N_v(t)$, is divided into susceptible sensitive ACP ($S_{v1}(t)$), susceptible resistant ACP ($S_{v2}(t)$), infected sensitive ACP ($I_{v1}(t)$), and infected resistant ACP ($I_{v2}(t)$), at any time t. Thus, $N_v(t) = S_{v1}(t) + S_{v2}(t) + I_{v1}(t) + I_{v2}(t)$.

We assume that the recruitment to the citrus population is by replanting at a rate proportional r to the difference between the actual number of citrus trees present N_h and maximum population size K. Resistant classes S_{v2} and $I_{v2}(t)$ are increased by sensitive vectors S_{v1} and $I_{v1}(t)$ who develop resistance at the rates φ_1 and φ_2, respectively. Moreover, let η_h the force of infection from ACP to trees and η_v the force of infection from trees to ACP. The HLB model incorporating resistance for ACP population is represented as a system of first order nonlinear ordinary differential equations as follows:

$$\begin{cases} \dfrac{dS_h}{dt} = r(K - N_h) + \omega_h V_h - \eta_h(t) S_h - (v_h + \mu_h) S_h, \\ \dfrac{dV_h}{dt} = v_h S_h - (1-\theta)\eta_h(t) V_h - (\omega_h + \mu_h) V_h, \\ \dfrac{dE_h}{dt} = \eta_h(t)(S_h + (1-\theta)V_h) - (\delta_h + \mu_h) E_h, \\ \dfrac{dI_h}{dt} = \delta_h E_h - (\gamma_h + \mu_h) I_h, \\ \dfrac{dS_{v1}}{dt} = \Lambda_1 - \eta_v(t) S_{v1} - (\varphi_1 + \mu_v) S_{v1}, \\ \dfrac{dS_{v2}}{dt} = \Lambda_2 - \eta_v(t) S_{v2} + \varphi_1 S_{v1} - \mu_v S_{v2}, \\ \dfrac{dI_{v1}}{dt} = \eta_v(t) S_{v1} - (\varphi_2 + \mu_v) I_{v1}, \\ \dfrac{dI_{v2}}{dt} = \eta_v(t) S_{v2} + \varphi_2 I_{v1} - \mu_v I_{v2}, \end{cases} \tag{2.1}$$

where

$$\eta_h(t) = \frac{b_v(\alpha_h I_{v1}(t) + \beta_h I_{v2}(t))}{N_h(t)}, \quad \text{and} \quad \eta_v(t) = \frac{b_v(\alpha_v E_h(t) + \beta_v I_h(t))}{N_h(t)}.$$

A schematic diagram of the model is depicted in Fig. 1, and the state variables and the parameters are described in Table 1. The basic qualitative properties of the model (2.1) will be explored in the subsequent section.

3. Model analysis

To better organize the analysis, we simplify some terms in the model by setting $d_1 = r + \mu_h$, $d_2 = \omega_h + \mu_h$, $d_3 = v_h + \mu_h$, $d_4 = \delta_h + \mu_h$, $d_5 = \gamma_h + \mu_h$, $d_6 = \varphi_1 + \mu_v$, $d_7 = \varphi_2 + \mu_v$, $d_8 = r + v_h + \mu_h$ and $d_9 = v_h + \omega_h + \mu_h$. We denote

$$G_h = \left\{ \left(S_h, V_h, E_h, I_h \right) \in R_+^4 : N_h \le \frac{rK}{d_1} \triangleq N_h^0 \right\},$$

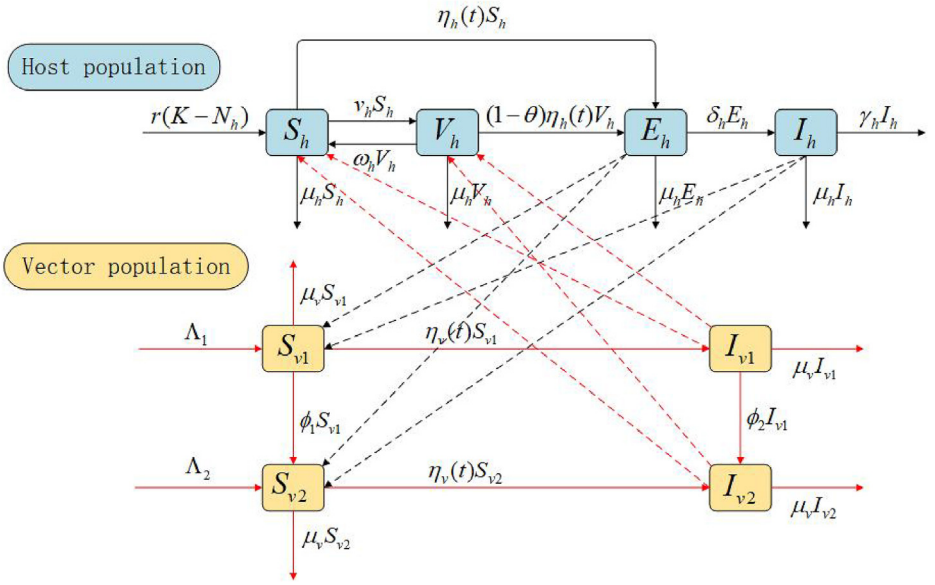

Fig. 1. Schematic Diagram of the HLB model (2.1).

Table 1
Description of The variables and their parameters for the HLB model (2.1).

Variable	Description
S_h	Population of susceptible citrus trees
V_h	Population of vaccinated citrus trees
E_h	Population of exposed citrus trees
I_h	Population of infected citrus trees
S_{v1}	Population of susceptible sensitive ACP
S_{v2}	Population of susceptible resistant ACP
I_{v1}	Population of infected sensitive ACP
I_{v2}	Population of infected resistant ACP
Parameter	**Description**
K	Environmental carrying capacity of citrus trees
r	Replanting rate of citrus trees
ω_h	Vaccine waning rate
b_v	ACP biting rate
α_h	Transmission probability from I_{v1} to S_h
β_h	Transmission probability from I_{v2} to S_h
ν_h	Vaccination rate
μ_h	Natural mortality rate in citrus trees
θ	Vaccine efficacy
δ_h	Disease progression rate of infectious of exposed citrus trees
γ_h	Disease related death rate
Λ_1	Sensitive ACP recruitment rate
Λ_2	Resistant ACP recruitment rate
α_v	Transmission probability from E_h to S_{v1} and S_{v2}
β_v	Transmission probability from I_h to S_{v1} and S_{v2}
μ_v	Natural mortality rate of ACP
φ_1	Mutation rate from susceptible sensitive ACP to susceptible resistant ACP
φ_2	Mutation rate from infected sensitive ACP to infected resistant ACP

$$G_v = \left\{ \left(S_{v1}, S_{v2}, I_{v1}, I_{v2} \right) \in R_+^4 : N_v \le \frac{\Lambda_1 + \Lambda_2}{\mu_v} \triangleq N_v^0 \right\}, \quad G = G_h \times G_v \subset R_+^8.$$

Lemma 3.1. Denote $\Gamma(t) = (S_h(t), V_h(t), E_h(t), I_h(t), S_{v1}(t), S_{v2}(t), I_{v1}(t), I_{v2}(t))^T$. Let the initial data $\Gamma(0) \gg 0$. Then the solutions $\Gamma(t)$ of the model (2.1) are non-negative for all $t > 0$. Furthermore

$$\underset{t\to\infty}{limsup} N_h(t) \le N_h^0, \lim_{t\to\infty} N_v(t) = N_v^0.$$

The region $G \subset R_+^8$ is positively-invariant for the model (2.1) with non-negative initial conditions.

Proof. Let the initial data of the model (2.1) $\Gamma(0) \gg 0$. It is obvious that $\frac{dS_h}{dt}_{S_h(t)=0} \ge \omega_h V_h \ge 0$, so we have $S_h(t) \ge 0$, for all $t > 0$. Similarly, we can get $V_h(t) \ge 0$, $E_h(t) \ge 0$, $I_h(t) \ge 0$, $S_{v1}(t) > 0$, $S_{v2}(t) > 0$, $I_{v1}(t) \ge 0$ and $I_{v2}(t) \ge 0$, for all $t > 0$.

Adding the first four equations of model (2.1), the total number of citrus trees N_h satisfies

$$\frac{dN_h}{dt} = r(K - N_h) - \mu_h N_h - \gamma_h I_h,$$

thus,

$$\frac{dN_h}{dt} \le r(K - N_h) - \mu_h N_h.$$

This implies that

$$\underset{t\to\infty}{limsup} N_h(t) \le N_h^0.$$

Adding the fifth to eighth equations of model (2.1), the total number of ACP N_v satisfies

$$\frac{dN_v}{dt} = \Lambda_1 + \Lambda_2 - \mu_v N_v,$$

thus,

$$\lim_{t\to\infty} N_v(t) = N_v^0.$$

Further, we know that $\frac{dN_h}{dt} \le 0$, if $N_h \ge N_h^0$ and $\frac{dN_v}{dt} \le 0$, if $N_v \ge N_v^0$. Therefore, the region G is positively-invariant. Clearly, the model (2.1) has a disease free equilibrium (DFE) point, $E_0 = (S_h^0, V_h^0, 0, 0, S_{v1}^0, S_{v2}^0, 0, 0)$, where

$$S_h^0 = \frac{d_2 N_h^0}{d_9} = \frac{d_2 rK}{d_9 d_1}, V_h^0 = \frac{\nu_h N_h^0}{d_9} = \frac{\nu_h rK}{d_9 d_1}, S_{v1}^0 = \frac{\Lambda_1}{d_6}, S_{v2}^0 = \frac{\Lambda_1 \varphi_1}{\mu_v d_6} + \frac{\Lambda_2}{\mu_v}.$$

Denote

$$k_1 = \frac{b_v \alpha_h S_h^0}{N_h^0}, \quad k_2 = \frac{b_v \beta_h S_h^0}{N_h^0}, \quad k_3 = \frac{(1-\theta) b_v \alpha_h V_h^0}{N_h^0}, \quad k_4 = \frac{(1-\theta) b_v \beta_h V_h^0}{N_h^0},$$
$$k_5 = \frac{b_v \alpha_v S_{v1}^0}{N_h^0}, \quad k_6 = \frac{b_v \beta_v S_{v1}^0}{N_h^0}, \quad k_7 = \frac{b_v \alpha_v S_{v2}^0}{N_h^0}, \quad k_8 = \frac{b_v \beta_v S_{v2}^0}{N_h^0}.$$

Then the Jacobian matrix of system (2.1) with respect to E_0 is

$$J(E_0) = \begin{pmatrix} J_{11} & J_{12} & 0 & -J_{14} \\ 0 & J_{22} & 0 & J_{24} \\ 0 & -J_{32} & J_{33} & 0 \\ 0 & J_{32} & 0 & J_{44} \end{pmatrix}, \tag{3.1}$$

where $J_{11} = \begin{pmatrix} -d_8 & -r+\omega_h \\ \nu_h & -d_2 \end{pmatrix}, J_{12} = \begin{pmatrix} -r & -r \\ 0 & 0 \end{pmatrix}, J_{14} = \begin{pmatrix} k_1 & k_2 \\ k_3 & k_4 \end{pmatrix}, J_{22} = \begin{pmatrix} -d_4 & 0 \\ \delta_h & -d_5 \end{pmatrix},$
$J_{24} = \begin{pmatrix} k_1+k_3 & k_2+k_4 \\ 0 & 0 \end{pmatrix}, J_{32} = \begin{pmatrix} k_5 & k_6 \\ k_7 & k_8 \end{pmatrix}, J_{33} = \begin{pmatrix} -d_6 & 0 \\ \varphi_1 & -\mu_v \end{pmatrix}, J_{44} = \begin{pmatrix} -d_7 & 0 \\ \varphi_2 & -\mu_v \end{pmatrix}.$

Denote

$$R_0 = \sqrt{\frac{(k_5 d_5 + k_6 \delta_h)(\mu_v(k_1+k_3) + \varphi_2(k_2+k_4)) + (k_7 d_5 + k_8 \delta_h)(k_2+k_4) d_7}{\mu_v d_4 d_5 d_7}}. \tag{3.2}$$

To better organize the analysis, we denote $p_0 = \mu_v d_4 d_5 d_7$, $p_1 = k_5 d_5 \mu_v (k_1+k_3)$, $p_2 = k_5 d_5 \varphi_2 (k_2+k_4)$, $p_3 = k_6 \delta_h \mu_v (k_1+k_3)$, $p_4 = k_6 \delta_h \varphi_2 (k_2+k_4)$, $p_5 = k_7 d_5 (k_2+k_4) d_7$, $p_6 = k_8 \delta_h (k_2+k_4) d_7$, and

$$A = \mu_v + d_4 + d_5 + d_7 > 0,$$

$$B = (\mu_v + d_7)d_4\left(1 - R_0^2\right) + \frac{p_1 + p_2 + p_3 + p_4 + p_6}{d_5 d_7} + \frac{p_2 + p_3 + p_4 + p_5 + p_6}{\mu_v d_5} + \mu_v(d_5 + d_7) + d_5(d_4 + d_7),$$

$$C = \left(\frac{p_0}{\mu_v} + \frac{p_0}{d_7} + \frac{p_0}{d_5}\right)\left(1 - R_0^2\right) + \frac{p_0}{d_4} + \frac{p_2 + p_4 + p_5 + p_6}{\mu_v} + \frac{p_3 + p_4 + p_6}{d_5} + \frac{p_1 + p_2 + p_3 + p_4}{d_7},$$

$$D = \mu_v d_4 d_5 d_7\left(1 - R_0^2\right) = p_0\left(1 - R_0^2\right),$$

$$Q_1 = \frac{p_2 + p_4 + p_5 + p_6}{\mu_v} + \frac{p_3 + p_4 + p_6}{d_5} + \frac{p_1 + p_2 + p_3 + p_4}{d_7} > 0,$$

$$Q_2 = (\mu_v + d_4)\frac{p_1 + p_2 + p_3 + p_4 + p_6}{d_5 d_7} + (d_4 + d_7)\frac{p_2 + p_3 + p_4 + p_5 + p_6}{\mu_v d_5} > 0,$$

$$Q_3 = (\mu_v + d_4)\mu_v d_4 + (d_4 + d_7)d_4 d_7 > 0,$$

$$Q_4 = \mu_v d_4(d_5 + d_7) + d_4 d_5 d_7 + \mu_v(d_5 + d_7)A + d_4 d_5(d_4 + d_5 + d_7) > 0,$$

$$Q_5 = \mu_v^3 d_4(d_5 + d_7)^2 + \mu_v^2 d_4\left(d_5^3 + 2d_4 d_5^2 + 2d_5^2 d_7 + 3d_4 d_5 d_7 + 2d_5 d_7^2 + 2d_4 d_7^2 + d_7^3\right)$$
$$+ \mu_v d_4 d_5\left(d_7^3 + 3d_4 d_7^2 + 3d_4 d_5 d_7 + d_4^2 d_5 + d_4 d_5^2\right) + d_4^2 d_5^2 d_7(d_4 + d_5 + 2d_7) > 0,$$

$$Q_6 = Q_3 Q_1 + Q_2\left(\frac{p_0}{\mu_v} + \frac{p_0}{d_7} + \frac{p_0}{d_5}\right) + Q_5 > 0,$$

Lemma 3.2. All eigenvalues of the matrix J(E_0) (3.1) have negative real parts if and only if $R_0 < 1$.

Proof. The characteristic equation of J_{11} is the following polynomial equation

$$\lambda^2 + (d_2 + d_8)\lambda + d_1 d_9 = 0. \tag{3.3}$$

According to Vieta theorem, the two roots of equation (3.3) are negative. It is easy to see that two eigenvalue of J_{33} are $-\mu_v$ and $-d_6$, which are negative. Denote

$$M = \begin{pmatrix} J_{22} & J_{24} \\ J_{32} & J_{44} \end{pmatrix} \tag{3.4}$$

We can see that all eigenvalues of the matrix M are the roots of the following quartic polynomial equation

$$\lambda^4 + A\lambda^3 + B\lambda^2 + C\lambda + D = 0.$$

Obviously, if $R_0 < 1$, then $B > 0$, $C > 0$ and $D > 0$. The Hertz determinants of the first to fourth order polynomial are as follows

$$\Delta_1 = A > 0,$$

$$\Delta_2 = AB - C$$
$$= Q_3\left(1 - R_0^2\right) + Q_2 + Q_4,$$

$$\Delta_3 = (AB - C)C - A^2D$$
$$= Q_3\left(\frac{p_0}{\mu_v} + \frac{p_0}{d_7} + \frac{p_0}{d_5}\right)\left(1 - R_0^2\right)^2 + Q_6\left(1 - R_0^2\right) + (Q_2 + Q_4)\left(\frac{p_0}{d_4} + Q_1\right),$$

$$\Delta_4 = D\Delta_3.$$

It is obvious that $\Delta_2 > 0$, $\Delta_3 > 0$ and $\Delta_4 > 0$ if $R_0 < 1$.By the criterion of Routh-Hurwitz, we obtain that all eigenvalues of M have negative real parts if and only if $R_0 < 1$. Therefore all eigenvalues of $J(E_0)$ have negative real parts if $R_0 < 1$.

Lemma 3.2 implies the following result holds.

Theorem 3.1. For system (2.1), the disease-free equilibrium E_0 is locally asymptotically stable if $R_0 < 1$ and unstable if $R_0 > 1$.

In order to analyze the permanence of system (2.1), we first give the following lemma.

Lemma 3.3. (See (Zhao, 2003)) Assume that

(I) $f(X_0) \subset X_0$ and f has a global attractor Ω.
(II) The maximal compact invariant set $\Omega_\partial = \Omega \cap M_\partial$ off in ∂X_0, possibly empty, has an acyclic covering $\tilde{M} = \{M_1, \ldots, M_k\}$ with the following properties:
  (a) M_i is isolated in $\tilde{X}$.
  (b) $W^s(M_i) \cap X_0 = \Phi$ for each $1 \le i \le k$.

Then f is uniformly persistent with respect to $(X_0, \partial X_0)$, i.e., there is $\eta > 0$ such that for any compact internally chain transitive set L with $L \not\subset \{M_i$, for all $1 \le i \le k\}$, $\inf_{x \in L} d(x, \partial X_0) > \eta$.

Theorem 3.2. If $R_0 > 1$, then system (2.1) is uniformly persistent.

Proof. We define $X = \{(S_h, V_h, E_h, I_h, S_{v1}, S_{v2}, I_{v1}, I_{v2}) \in R^8$: $S_h \ge 0$, $V_h \ge 0$, $E_h \ge 0$, $I_h \ge 0$, $S_{v1} \ge 0$, $S_{v2} \ge 0$, $I_{v1} \ge 0$, $I_{v2} \ge 0\}$, $X_0 = \{(S_h, V_h, E_h, I_h, S_{v1}, S_{v2}, I_{v1}, I_{v2}) \in X$: $E_h > 0$, $I_h > 0$, $I_{v1} > 0$, $I_{v2} > 0\}$, and $\partial X_0 = X \setminus X_0$.

In order to show that system (2.1) is uniformly persistent, we only need to prove that ∂X_0 repels uniformly the solutions of X_0. Obviously, both X and X_0 are positively invariant and ∂X_0 is relatively closed in X and (2.1) is point dissipative. Let

$$M_\partial = \{(S_h(0), V_h(0), E_h(0), I_h(0), S_{v1}(0), S_{v2}(0), I_{v1}(0), I_{v2}(0)) \in \partial X_0 : (S_h(t), V_h(t), E_h(t), I_h(t), S_{v1}(t), S_{v2}(t), I_{v1}(t), I_{v2}(t)) \in \partial X_0, \forall\, t \ge 0\}$$

We now show that

$$M_\partial = \{(S_h(t), V_h(t), 0, 0, S_{v1}(t), S_{v2}(t), 0, 0) \in X : S_h(t) \ge 0, V_h(t) \ge 0, S_{v1}(t) \ge 0, S_{v2}(t) \ge 0\} \tag{3.5}$$

Assume $(S_h(0), V_h(0), E_h(0), I_h(0), S_{v1}(0), S_{v2}(0), I_{v1}(0), I_{v2}(0)) \in M_\partial$. It suffices to show that $E_h(t) = 0$, $I_h(t) = 0$, $I_{v1}(t) = 0$ and $I_{v2}(t) = 0$ for all $t \ge 0$. Suppose not. Then there exists a $t_0 \ge 0$ such that $E_h(t_0), I_h(t_0), I_{v1}(t_0), I_{v2}(t_0)$ at least one is greater than 0. Without loss of generality, we only discuss the case $E_h(t_0) > 0$, $S_h(t_0) = 0$, $V_h(t_0) = 0$, $I_h(t_0) = 0$, $S_{v1}(t_0) = 0$, $S_{v2}(t_0) = 0$, $I_{v1}(t_0) = 0$ and $I_{v2}(t_0) = 0$. Since

$$\frac{dI_h}{dt}|_{t=t_0} = \delta_h E_h(t_0) > 0, \quad \frac{dS_{v1}}{dt}|_{t=t_0} = \Lambda_1 > 0, \quad \frac{dS_{v2}}{dt}|_{t=t_0} = \Lambda_2 > 0, \quad \frac{dE_h}{dt}|_{t=t_0} > -d_4 E_h,$$

it follows that there is an $\epsilon_0 > 0$ small enough such that $S_{v1}(t) > 0$, $S_{v2}(t) > 0$, $E_h(t) > 0$ and $I_h(t) > 0$ for all $t_0 < t < t_0 + \epsilon_0$. Furthermore, let $t_1 = t_0 + \frac{\epsilon_0}{2}$, then we have $S_{v1}(t_1) > 0$, $S_{v2}(t_1) > 0$, $E_h(t_1) > 0$ and $I_h(t_1) > 0$. If $I_{v1}(t_1) > 0$, then

$$\frac{dI_{v1}}{dt}|_{t=t_1} > -(\varphi_2 + \mu_v)I_{v1},$$

this implies that $I_{v1}(t) > 0$ for all $t \geq t_1$. If $I_{v1}(t_1) = 0$, we get

$$\frac{dI_{v1}}{dt}|_{t=t_1} = \eta_v(t)(t_1)S_{v1}(t_1) > 0,$$

It then follows that there is an ϵ_1 $(0 < \epsilon_1 < \frac{\epsilon_0}{2})$ such that $I_{v1}(t) > 0$ for all $t_1 < t < t_1 + \epsilon_1$. Similarly, we can show that there exists an ϵ_2 $(0 < \epsilon_2 < \frac{\epsilon_1}{2})$ such that $I_{v2}(t) > 0$ for all $t \in (t_1 + \frac{\epsilon_1}{2}, t_1 + \frac{\epsilon_1}{2} + \epsilon_2)$, respectively. Thus, for all $t_1 + \frac{\epsilon_1}{2} < t < t_1 + \frac{\epsilon_1}{2} + \epsilon_2$ we have $E_h(t) > 0$, $I_h(t) > 0$, $I_{v1}(t) > 0$ and $I_{v2}(t) > 0$. This contradicts the assumption that $(S_h(0), V_h(0), E_h(0), I_h(0), S_{v1}(0), S_{v2}(0), I_{v1}(0), I_{v2}(0)) \notin M_\partial$. Thus (3.5) holds.

It is obvious that $E_0 = (S_h^0, V_h^0, 0, 0, S_{v1}^0, S_{v2}^0, 0, 0)$ is the unique equilibrium in M_∂. We now demonstrate that E_0 repels the solutions in X_0.

By the proof of Lemma 3.2, we know that $det(M) < 0$ provided that $R_0 > 1$, here M is defined in (3.4). Therefore, if $R_0 > 1$, then there exist $\zeta_1 > 0$ and $\zeta_2 > 0$ small enough such that

$$(\bar{k}_5 d_5 + \bar{k}_6 \delta_h)(\mu_v(\bar{k}_1 + \bar{k}_3) + \varphi_2(\bar{k}_2 + \bar{k}_4)) + (\bar{k}_7 d_5 + \bar{k}_8 \delta_h)(\bar{k}_2 + \bar{k}_4)d_7 > \mu_v d_4 d_5 d_7, \tag{3.6}$$

$$det(\tilde{M}) = det\begin{pmatrix} J_{22} & \bar{J}_{24}\bar{J}_{32}J_{44} \end{pmatrix} < 0, \tag{3.7}$$

and

$$\begin{aligned}
&\tilde{S}_h^0 \doteq \frac{d_2 rK + (1-\theta)\tilde{\eta}_h rK - 2d_2 r\zeta_2 - 2r(1-\theta)\tilde{\eta}_h\zeta_2}{d_1 d_9 + (1-\theta)\tilde{\eta}_h d_8 + d_2\tilde{\eta}_h + (1-\theta)\tilde{\eta}_h{}^2} > S_h^0 - \zeta_1,\\
&\tilde{v}_h^0 \doteq \frac{v_h rK - 2rv_h\zeta_2}{d_1 d_9 + (1-\theta)\tilde{\eta}_h d_8 + d_2\tilde{\eta}_h + (1-\theta)\tilde{\eta}_h{}^2} > V_h^0 - \zeta_1,\\
&\tilde{S}_{v1}^0 \doteq \frac{\Lambda_1}{\tilde{\eta}_v + \varphi_1 + \mu_v} > S_{v1}^0 - \zeta_1,\\
&\tilde{S}_{v2}^0 \doteq \frac{\Lambda_2 + \varphi_1\tilde{S}_{v1}^0}{\tilde{\eta}_v + \mu_v} > S_{v2}^0 - \zeta_1,
\end{aligned} \tag{3.8}$$

hold, where $\bar{k}_1 = \frac{b_v\alpha_h}{N_h^0}(S_h^0 - \zeta_1)$, $\bar{k}_2 = \frac{b_v\beta_h}{N_h^0}(S_h^0 - \zeta_1)$, $\bar{k}_3 = \frac{(1-\theta)b_v\alpha_h}{N_h^0}(V_h^0 - \zeta_1)$, $\bar{k}_4 = \frac{(1-\theta)b_v\beta_h}{N_h^0}(V_h^0 - \zeta_1)$, $\bar{k}_5 = \frac{b_v\alpha_v}{N_h^0}(S_{v1}^0 - \zeta_1)$, $\bar{k}_6 = \frac{b_v\beta_v}{N_h^0}(S_{v1}^0 - \zeta_1)$, $\bar{k}_7 = \frac{b_v\alpha_v}{N_h^0}(S_{v2}^0 - \zeta_1)$, $\bar{k}_8 = \frac{b_v\beta_v}{N_h^0}(S_{v2}^0 - \zeta_1)$, $\tilde{N}_h = \frac{rK - \gamma_h\zeta_2}{d_1}$, $\tilde{\eta}_h = \frac{b_v(\alpha_h\zeta_2 + \beta_h\zeta_2)}{\tilde{N}_h}$, $\tilde{\eta}_v = \frac{b_v(\alpha_v\zeta_2 + \beta_v\zeta_2)}{\tilde{N}_h}$, and

$$\bar{J}_{24} = \begin{pmatrix} \bar{k}_1 + \bar{k}_3 & \bar{k}_2 + \bar{k}_4 & 0 & 0 \end{pmatrix}, \bar{J}_{32} = \begin{pmatrix} \bar{k}_5 & \bar{k}_6 \\ \bar{k}_7 & \bar{k}_8 \end{pmatrix}$$

Suppose $(S_h(t), V_h(t), E_h(t), I_h(t), S_{v1}(t), S_{v2}(t), I_{v1}(t), I_{v2}(t))$ is a solution of system (2.1) with initial value $(S_h(0), V_h(0), E_h(0), I_h(0), S_{v1}(0), S_{v2}(0), I_{v1}(0), I_{v2}(0)) \in X_0$. We now claim that

$$\limsup_{t\to\infty} \max\{E_h(t), I_h(t), I_{v1}(t), I_{v2}(t)\} > \zeta_2. \tag{3.9}$$

Suppose that the claim is not valid. Then there is a $T_0 > 0$ such that

$$E_h(t) \le \zeta_2, \quad I_h(t) \le \zeta_2, \quad I_{v1}(t) \le \zeta_2, \quad I_{v2}(t) \le \zeta_2, \quad \text{for all } t \ge T_0. \tag{3.10}$$

It follows from system (2.1) and (3.10) that

$$\frac{dN_h}{dt} \ge r(K - N_h) - \mu_h N_h - \gamma_h \zeta_2.$$

Thus, there exists a $T_1 > T_0$ such that

$$N_h > \frac{rK - \gamma_h \zeta_2}{d_1} = \tilde{N}_h \quad \text{for all } t \ge T_1. \tag{3.11}$$

From the first and second equations of the model (2.1) and (3.11), we have

$$\begin{cases} \dfrac{dS_h}{dt} \ge r(K - S_h - V_h - 2\zeta_2) + \omega_h V_h - \tilde{\eta}_h S_h - d_3 S_h, \\ \dfrac{dV_h}{dt} \ge \nu_h S_h - (1-\theta)\tilde{\eta}_h V_h - d_2 V_h, \end{cases}$$

for $t \ge T_1$. Consider the following comparison system

$$\begin{cases} \dfrac{d\tilde{S}_h}{dt} = r(K - \tilde{S}_h - \tilde{V}_h - 2\zeta_2) + \omega_h \tilde{V}_h - \tilde{\eta}_h \tilde{S}_h - d_3 \tilde{S}_h, \\ \dfrac{d\tilde{V}_h}{dt} = \nu_h \tilde{S}_h - (1-\theta)\tilde{\eta}_h \tilde{V}_h - d_2 \tilde{V}_h. \end{cases} \tag{3.12}$$

We can restrict ζ_2 to be small enough such that system (3.12) admits a unique positive equilibrium $(\tilde{S}_h^0, \tilde{V}_h^0)$, which is globally asymptotically stable (the proof is stated in Appendix A). By the comparison principle in differential equations and (3.8), there is a $T_2 > 0$ such that

$$S_h(t) \ge S_h^0 - \zeta_1, \quad V_h(t) \ge V_h^0 - \zeta_1, \quad \text{for } t > T_2. \tag{3.13}$$

From the fifth equation of system (2.1) and (3.11), we get

$$\frac{dS_{v1}}{dt} \ge \Lambda_1 - \tilde{\eta}_v S_{v1} - (\varphi_1 + \mu_v) S_{v1},$$

for $t \ge T_1$. According to the comparison principle and (3.8), there exists a $T_3 > T_2$, such that

$$S_{v1}(t) > S_{v1}^0 - \zeta_1, \quad \text{for } t \ge T_3. \tag{3.14}$$

It follows from the sixth equation of system (2.1), (3.11) and (3.14) that

$$\frac{dS_{v2}}{dt} \ge \Lambda_2 - \tilde{\eta}_v S_{v2} + \varphi_1 \tilde{S}_{v1}^0 - \mu_v S_{v2},$$

for $t \ge T_3$. Then, there exists a $T_4 > T_3$, such that

$$S_{v2}(t) > S_{v2}^0 - \zeta_1, \quad \text{for } t \ge T_4. \tag{3.15}$$

Consequently, from system (2.1) and (3.13)–(3.15), we obtain that for $t > T_4$,

$$\begin{cases} \dfrac{dE_h}{dt} \geq \dfrac{b_v(\alpha_h I_{v1} + \beta_h I_{v2})}{N_h^0}((S_h^0 - \zeta_1) + (1-\theta)(V_h^0 - \zeta_1)) - d_4 E_h, \\ \dfrac{dI_h}{dt} \geq \delta_h E_h - d_5 I_h, \\ \dfrac{dI_{v1}}{dt} \geq \dfrac{b_v(\alpha_v E_h + \beta_v I_h)}{N_h^0}(S_{v1}^0 - \zeta_1) - (\varphi_2 + \mu_v) I_{v1}, \\ \dfrac{dI_{v2}}{dt} \geq \dfrac{b_v(\alpha_v E_h + \beta_v I_h)}{N_h^0}(S_{v2}^0 - \zeta_1) + \varphi_2 I_{v1} - \mu_v I_{v2}. \end{cases}$$

Consider the following auxiliary system:

$$\begin{cases} \dfrac{d\bar{E}_h}{dt} = \dfrac{b_\upsilon\left(\alpha_h \bar{I}_{\upsilon 1} + \beta_h \bar{I}_{\upsilon 2}\right)}{N_h^0}\left(\left(S_h^0 - \zeta_1\right) + (1-\theta)\left(V_h^0 - \zeta_1\right)\right) - d_4 \bar{E}_h, \\ \dfrac{d\bar{I}_h}{dt} = \delta_h \bar{E}_h - d_5 \bar{I}_h, \\ \dfrac{d\bar{I}_{\upsilon 1}}{dt} = \dfrac{b_\upsilon\left(\alpha_\upsilon \bar{E}_h + \beta_\upsilon \bar{I}_{\mathrm{h}}\right)}{N_h^0}\left(S_{\upsilon 1}^0 - \zeta_1\right) - (\phi_2 + \mu_\upsilon)\bar{I}_{\upsilon 1}, \\ \dfrac{d\bar{I}_{\upsilon 2}}{dt} = \dfrac{b_\upsilon\left(\alpha_\upsilon \bar{E}_h + \beta_\upsilon \bar{I}_{\mathrm{h}}\right)}{N_h^0}\left(S_{\upsilon 2}^0 - \zeta_1\right) + \phi_2 + \bar{I}_{\upsilon 1} - \mu_\upsilon \bar{I}_{\upsilon 2}. \end{cases} \tag{3.16}$$

Obviously, system (3.16) has zero equilibrium point. By simple calculation, we obtain that the Jacobian matrix of system (3.16) at zero equilibrium point is $\tilde{M}$ (defined in (3.7)). Since $\tilde{M}$ admits positive off-diagonal elements, by Perron-Frobenius Theorem, we can see that there exists a positive eigenvector $v_{\tilde{M}}$ for the maximin eigenvalue $\lambda_{\tilde{M}}$ of $\tilde{M}$. Extensive calculations yield that $\lambda_M > 0$ since (3.6) and (3.7) hold. Consequently, we can get $\lim_{t\to\infty} \bar{E}_h(t) = \infty$, $\lim_{t\to\infty} \bar{I}_h(t) = \infty$, $\lim_{t\to\infty} \bar{I}_{v1}(t) = \infty$, $\lim_{t\to\infty} \bar{I}_{v2}(t) = \infty$. Furthermore, by the comparison principle, we obtain $\lim_{t\to\infty} E_h(t) = \infty$, $\lim_{t\to\infty} I_h(t) = \infty$, $\lim_{t\to\infty} I_{v1}(t) = \infty$, $\lim_{t\to\infty} I_{v2}(t) = \infty$. This contradicts $E_h(t) \leq \zeta_2$, $I_h(t) \leq \zeta_2$, $I_{v1}(t) \leq \zeta_2$, $I_{v2}(t) \leq \zeta_2$, for all $t \geq T_0$. Hence, (3.9) holds and the claim is proved. This indicates $W^s(E_0) \cap X_0 = \Phi$. Obviously, every forward orbit in M_∂ converges to E_0. It follows from Lemma 3.3 that system (2.1) is uniformly persistent with respect to $(X_0, \partial X_0)$. This completes the proof.

4. Optimal control

Insecticide applications and removing infected trees are two tactics being employed for the control of HLB (Bovè, 2006; Gottwald, 2010). There is an urgent need to explore an optimal control strategy in terms of possible combination of strategies to prevent the spread of citrus HLB while minimizing the implementation cost. In this paper, we introduce into the transmission model (2.1) a time dependent control variable $u_h(t)$, representing removing effort of infected citrus trees, and also consider a time dependent control variable $u_v(t)$, representing killing effort of sensitive ACP and resistant ACP. Thus, model (2.1) with the time dependent control variables $u_h(t)$ and $u_v(t)$ becomes:

$$\begin{cases} \dfrac{dS_h}{dt} = r(K - N_h) + \omega_h V_h - \eta_h(t) S_h - d_3 S_h, \\ \dfrac{dV_h}{dt} = v_h S_h - (1-\theta)\eta_h(t) V_h - d_2 V_h, \\ \dfrac{dE_h}{dt} = \eta_h(t)(S_h + (1-\theta)V_h) - d_4 E_h, \\ \dfrac{dI_h}{dt} = \delta_h E_h - (\rho_1 u_h(t) + d_5) I_h, \\ \dfrac{dS_{v1}}{dt} = \Lambda_1 - \eta_v(t) S_{v1} - (\mu_v + \rho_2 u_v(t)) S_{v1} - \varphi_1 S_{v1}, \\ \dfrac{dS_{v2}}{dt} = \Lambda_2 - \eta_v(t) S_{v2} - (\mu_v + \rho_3 u_v(t)) S_{v2} + \varphi_1 S_{v1}, \\ \dfrac{dI_{v1}}{dt} = \eta_v(t) S_{v1} - (\mu_v + \rho_2 u_v(t)) I_{v1} - \varphi_2 I_{v1}, \\ \dfrac{dI_{v2}}{dt} = \eta_v(t) S_{v2} - (\mu_v + \rho_3 u_v(t)) I_{v2} + \varphi_2 I_{v1}, \end{cases} \tag{4.1}$$

where ρ_1, ρ_2, ρ_3 is the control intensity coefficient. Our goal is to minimize the cost function defined as

$$J(u) = \int_0^{t_f} \{A_1 E_h(t) + A_2 I_h(t) + A_3 N_v(t) + A_4 u_h^2(t) + A_5 u_v^2(t)\} dt \tag{4.2}$$

subject to system (4.1), where t_f is the control period. This performance specification involves minimizing the numbers of exposed and infected citrus tree, along with the cost of applying the controls $u(t) = (u_h(t), u_v(t))$. The quadratic costs have been frequently used (Agusto, 2013; Pei et al., 2016; Zhang et al., 2020). The coefficients, A_i, $i = 1, \ldots, 5$ represent the desired weights on the benefit and cost the controls $u(t) = (u_h(t), u_v(t))$ is a bounded Lebesgue integrable functions (Agusto & Lenhart, 2013; Pei et al., 2016). And we need to find an optimal control $u^* = (u_h^*, u_v^*)$, such that

$$J(u^*) = \min_U J(u),$$

where the control set,

$$U = \{u(t) : [0, t_f] \to [0,1] \times [0,1]\}, \tag{4.3}$$

where $u(t)$ is Lebesgue measurable. The necessary conditions that an optimal control quintuple must satisfy derive from the Pontryagin's Minimum Principle (Pontryagin, 2018). This principle converts (4.1) and (4.2) into a problem of minimizing pointwise a Hamiltonian H, with respect to the controls $u_h(t)$ and $u_v(t)$. In order to obtain the optimality conditions, we first formulate the following Hamilton functional from the objective functional (4.2) and the governing dynamics (4.1):

$$\begin{aligned} H = {} & A_1 E_h(t) + A_2 I_h(t) + A_3 N_v(t) + A_4 u_h^2(t) + A_5 u_v^2(t) \\ & + \lambda_{S_h}[r(K - N_h) + \omega_h V_h - \eta_h(t) S_h - d_3 S_h] \\ & + \lambda_{V_h}[v_h S_h - (1-\theta)\eta_h(t) V_h - d_2 V_h] \\ & + \lambda_{E_h}[\eta_h(t)(S_h + (1-\theta)V_h) - d_4 E_h] \\ & + \lambda_{I_h}[\delta_h E_h - (\rho_1 u_h(t) + \mu_h) I_h] \\ & + \lambda_{S_{v1}}[\Lambda_1 - \eta_v(t) S_{v1} - (\mu_v + \rho_2 u_v(t)) S_{v1} - \varphi_1 S_{v1}] \\ & + \lambda_{S_{v2}}[\Lambda_2 - \eta_v(t) S_{v2} - (\mu_v + \rho_3 u_v(t)) S_{v2} + \varphi_1 S_{v1}] \\ & + \lambda_{I_{v1}}[\eta_v(t) S_{v1} - (\mu_v + \rho_2 u_v(t)) I_{v1} - \varphi_2 I_{v1}] \\ & + \lambda_{I_{v2}}[\eta_v(t) S_{v2} - (\mu_v + \rho_3 u_v(t)) I_{v2} + \varphi_2 I_{v1}]. \end{aligned} \tag{4.4}$$

where $\lambda_{S_h}, \lambda_{V_h}, \lambda_{E_h}, \lambda_{I_h}, \lambda_{S_{v1}}, \lambda_{S_{v2}}, \lambda_{I_{v1}}, \lambda_{I_{v2}}$ are the associated adjoints for the states $S_h, V_h, E_h, I_h, S_{v1}, S_{v2}, I_{v1}, I_{v2}$. The system of adjoint equations is found by taking the appropriate partial derivatives of the Hamiltonian (4.4) with respect to the associated state and control variables.

Theorem 4.1. Given an optimal control variables (u_h^*, u_v^*), and solutions $S_h^*, V_h^*, E_h^*, I_h^*, S_{v1}^*, S_{v2}^*, I_{v1}^*, I_{v2}^*$ of the corresponding state system (4.1) that minimizes $J(u_h^*, u_v^*)$ over U . Then there exists adjoint variables $\lambda_{S_h}, \lambda_{V_h}, \lambda_{E_h}, \lambda_{I_h}, \lambda_{S_{v1}}, \lambda_{S_{v2}}, \lambda_{I_{v1}}, \lambda_{I_{v2}}$ satisfying

$$-\frac{d\lambda_i}{dt} = \frac{\partial H}{\partial i}. \tag{4.5}$$

and with transversality conditions

$$\lambda_i(t_f) = 0, \text{where } i = S_h, V_h, E_h, I_h, S_{v1}, S_{v2}, I_{v1}, I_{v2}. \tag{4.6}$$

The optimality conditions is given as

$$\frac{\partial H}{\partial u_j} = 0, j = h, v.$$

Furthermore, *the time dependent control variables* (u_h^*, u_v^*) *are given as*

$$\begin{cases} u_h^* = \max\left\{0, \min\left\{\frac{\lambda_{I_h}\rho_1 I_h^*}{2A_4}, 1\right\}\right\}, \\ u_v^* = \max\left\{0, \min\left\{\frac{\lambda_{S_{v1}}\rho_2 S_{v1}^* + \lambda_{S_{v2}}\rho_3 S_{v2}^* + \lambda_{I_{v1}}\rho_2 I_{v1}^* + \lambda_{I_{v2}}\rho_3 I_{v2}^*}{2A_5}, 1\right\}\right\} \end{cases} \tag{4.7}$$

Proof. According to the result in (Fleming & Rishel, 2012), we can easily obtain the existence of an optimal control. Consequently, the differential equations governing the adjoint variables are obtained by the differentiation of the Hamiltonian function, evaluated at the optimal controls. Then the adjoint system yields:

$$\begin{aligned}
-\frac{d\lambda_{S_h}}{dt} &= \frac{\partial H}{\partial S_h}, \quad \lambda_{S_h}(t_f) = 0, \\
-\frac{d\lambda_{V_h}}{dt} &= \frac{\partial H}{\partial V_h}, \quad \lambda_{V_h}(t_f) = 0, \\
-\frac{d\lambda_{E_h}}{dt} &= \frac{\partial H}{\partial E_h}, \quad \lambda_{E_h}(t_f) = 0, \\
-\frac{d\lambda_{I_h}}{dt} &= \frac{\partial H}{\partial I_h}, \quad \lambda_{I_h}(t_f) = 0, \\
-\frac{d\lambda_{S_{v1}}}{dt} &= \frac{\partial H}{\partial S_{v1}}, \quad \lambda_{S_{v1}}(t_f) = 0, \\
-\frac{d\lambda_{S_{v2}}}{dt} &= \frac{\partial H}{\partial S_{v2}}, \quad \lambda_{S_{v2}}(t_f) = 0, \\
-\frac{d\lambda_{I_{v1}}}{dt} &= \frac{\partial H}{\partial I_{v1}}, \quad \lambda_{I_{v1}}(t_f) = 0, \\
-\frac{d\lambda_{I_{v2}}}{dt} &= \frac{\partial H}{\partial I_{v2}}, \quad \lambda_{I_{v2}}(t_f) = 0.
\end{aligned}$$

Evaluated at the optimal controls and corresponding state variables, results in the stated adjoint system (4.4) and (4.5) given by

$$\frac{d\lambda_{S_h}}{dt} = \lambda_{S_h}(r+d_3) - \lambda_{V_h}\nu_h + \eta_h(t)^*\frac{N_h^* - S_h^*}{N_h^*}(\lambda_{S_h} - \lambda_{E_h}) - \eta_h(t)^*\frac{(1-\theta)V_h^*}{N_h^*}(\lambda_{V_h} - \lambda_{E_h})$$
$$- \eta_v(t)^*\frac{S_{v1}^*}{N_h^*}(\lambda_{S_{v1}} - \lambda_{I_{v1}}) - \eta_v(t)^*\frac{S_{v2}^*}{N_h^*}(\lambda_{S_{v2}} - \lambda_{I_{v2}}),$$

$$\frac{d\lambda_{V_h}}{dt} = \lambda_{S_h}(r-\omega_h) + \lambda_{V_h}d_2 - \eta_h(t)^*\frac{S_h^*}{N_h^*}(\lambda_{S_h} - \lambda_{E_h}) + (1-\theta)\eta_h(t)^*\frac{N_h^* - V_h^*}{N_h^*}(\lambda_{V_h} - \lambda_{E_h})$$
$$- \eta_v(t)^*\frac{S_{v1}^*}{N_h^*}(\lambda_{S_{v1}} - \lambda_{I_{v1}}) - \eta_v(t)^*\frac{S_{v2}^*}{N_h^*}(\lambda_{S_{v2}} - \lambda_{I_{v2}}),$$

$$\frac{d\lambda_{E_h}}{dt} = -A_1 + \lambda_{S_h}r + \lambda_{E_h}d_4 - \lambda_{I_h}\delta_h - \eta_h(t)^*\frac{S_h^*}{N_h^*}(\lambda_{S_h} - \lambda_{E_h}) - (1-\theta)\eta_h(t)^*\frac{V_h^*}{N_h^*}(\lambda_{V_h} - \lambda_{E_h})$$
$$- (\eta_v(t)^* - b_v\alpha_v)\frac{S_{v1}^*}{N_h^*}(\lambda_{S_{v1}} - \lambda_{I_{v1}}) - (\eta_v(t)^* - b_v\alpha_v)\frac{S_{v2}^*}{N_h^*}(\lambda_{S_{v2}} - \lambda_{I_{v2}}),$$

$$\frac{d\lambda_{I_h}}{dt} = -A_2 + \lambda_{S_h}r + \lambda_{I_h}(\rho_1 u_h + \mu_h) - \eta_h(t)^*\frac{S_h^*}{N_h^*}(\lambda_{S_h} - \lambda_{E_h}) - (1-\theta)\eta_h(t)^*\frac{V_h^*}{N_h^*}(\lambda_{V_h} - \lambda_{E_h})$$
$$- (\eta_v(t)^* - b_v\beta_v)\frac{S_{v1}^*}{N_h^*}(\lambda_{S_{v1}} - \lambda_{I_{v1}}) - (\eta_v(t)^* - b_v\beta_v)\frac{S_{v2}^*}{N_h^*}(\lambda_{S_{v2}} - \lambda_{I_{v2}}),$$

$$\frac{d\lambda_{S_{v1}}}{dt} = -A_3 + \lambda_{S_{v1}}(\rho_2 u_v + \mu_v) + \varphi_1(\lambda_{S_{v1}} - \lambda_{S_{v2}}) + \eta_v(t)^*(\lambda_{S_{v1}} - \lambda_{I_{v1}}),$$

$$\frac{d\lambda_{S_{v2}}}{dt} = -A_3 + \lambda_{S_{v2}}(\rho_3 u_v + \mu_v) + \eta_v(t)^*(\lambda_{S_{v2}} - \lambda_{I_{v2}}),$$

$$\frac{d\lambda_{I_{v1}}}{dt} = -A_3 + \lambda_{I_{v1}}(\rho_2 u_v + \mu_v) + \varphi_2(\lambda_{I_{v1}} - \lambda_{I_{v2}}) + \frac{b_v\alpha_h S_h^*}{N_h^*}(\lambda_{S_h} - \lambda_{E_h}) + \frac{(1-\theta)b_v\alpha_h V_h^*}{N_h^*}(\lambda_{V_h} - \lambda_{E_h}),$$

$$\frac{d\lambda_{I_{v2}}}{dt} = -A_3 + \lambda_{I_{v2}}(\rho_3 u_v + \mu_v) + \frac{b_v\beta_h S_h^*}{N_h^*}(\lambda_{S_h} - \lambda_{E_h}) + \frac{(1-\theta)b_v\beta_h V_h^*}{N_h^*}(\lambda_{V_h} - \lambda_{E_h}),$$

In addition, differentiating the Hamiltonian functional with respect to the control variables in the interior of the control set U, and then solving for controls (u_h^*, u_v^*) result in the optimality conditions given as follows:

$$\begin{aligned}\frac{\partial H}{\partial u_h} &= 2A_4u_h - \lambda_{I_h}\rho_1 I_h^*,\\ \frac{\partial H}{\partial u_v} &= 2A_5u_v - \lambda_{S_{v1}}\rho_2 S_{v1}^* - \lambda_{S_{v2}}\rho_3 S_{v2}^* - \lambda_{I_{v1}}\rho_2 I_{v1}^* - \lambda_{I_{v2}}\rho_3 I_{v2}^*.\end{aligned} \tag{4.8}$$

By simple calculation, we have

$$\begin{cases} u_h^* &= \dfrac{\lambda_{I_h}\rho_1 I_h^*}{2A_4},\\ u_v^* &= \dfrac{\lambda_{S_{v1}}\rho_2 S_{v1}^* + \lambda_{S_{v2}}\rho_3 S_{v2}^* + \lambda_{I_{v1}}\rho_2 I_{v1}^* + \lambda_{I_{v2}}\rho_3 I_{v2}^*}{2A_5}. \end{cases} \tag{4.9}$$

Taking into account the property of control set in (4.3), the characterization (4.6) can be obtained. This completes the proof.

In the next part, we will simulate numerically the solutions of the optimality system and the corresponding optimal control, and then give the interpretations from various cases.

5. Numerical simulation

In this section, we mainly present some numerical simulation results to verify or extend our results, which explore the impact of insecticides resistance on HLB transmission between citrus tree population and ACP population, and assess the effects of different control strategies against HLB. By using the Latin Hypercube Sampling (LHS) method (Blower & Dowlatabadi, 1994) and the forward-backward sweep method (Lenhart & Workman, 2007). Table 2 contains the value of the parameters that will be used in numerical simulations.

To examine the sensitivity of model results to the uncertainty of parameters, we do sensitivity and uncertainty analysis. Based on the parameters of model (2.1), we perform a global sensitivity analysis on the basic reproduction number R_0. By using the Latin Hypercube Sampling (LHS) method (Blower & Dowlatabadi, 1994), we compute the Partial Rank Correlation Coefficients (PRCCs) of R_0. The sensitivity and uncertainty analysis are presented in Fig. 2. It shows how uncertainty in model parameters may influence R_0. We can observe from Fig. 2(a) that R_0 is very sensitive to environmental carrying capacity of citrus trees K, ACP biting rate b_v, Vaccination rate ν_h, transmission probability from ACP to citrus trees α_h and β_h, vaccine efficacy θ, disease related death rate γ_h, ACP recruitment rate Λ_1 and Λ_2, transmission probability from I_h to ACP β_v, natural mortality rate of ACP μ_v, but not sensitive to replanting rate of citrus trees r, natural mortality rate in citrus trees μ_h, disease progression rate of infectious of exposed citrus trees δ_h, transmission probability from E_h to ACP α_v, mutation rate from sensitive ACP to infected resistant ACP φ_1 and φ_2. For both transmission probabilities, β_v has a greater impact on R_0. Thus, decreasing β_v is very effective in reducing R_0, that is to say, decreasing the transmission probability from I_h to ACP plays a key role in the control of HLB. Fig. 2(b) (uncertainty analysis), we can see that about 88.7% of the distribution of R_0 is greater than 1.

Table 2
Numerical values of the parameters for HLB model (2.1).

Parameter	Baseline value	Unit	Reference
K	1000	–	Zhang et al. (2020)
r	0.6	$year^{-1}$	Zhang et al. (2020)
ω_h	0.05	$year^{-1}$	Assumed
b_v	600	$year^{-1}$	Assumed
α_h	4.8830×10^{-4}	–	Taylor et al. (2016)
β_h	$0.8 \times 4.8830 \times 10^{-4}$	–	Assumed
ν_h	0.7	$year^{-1}$	Assumed
μ_h	0.04	$year^{-1}$	Mingxue (2009)
θ	0.8	–	Assumed
δ_h	12.97	$year^{-1}$	Chiyaka et al. (2012)
γ_h	0.1	$year^{-1}$	Assumed
Λ_1	3.3253×10^5	$year^{-1}$	Taylor et al. (2016)
Λ_2	$0.8 \times 3.3253 \times 10^5$	$year^{-1}$	Assumed
α_v	$0.9 \times 3.9064 \times 10^{-4}$	–	Assumed
β_v	3.9064×10^{-4}	–	Taylor et al. (2016)
μ_v	5.9441	$year^{-1}$	Taylor et al. (2016)
φ_1	0.3	$year^{-1}$	Assumed
φ_2	0.24	$year^{-1}$	Assumed

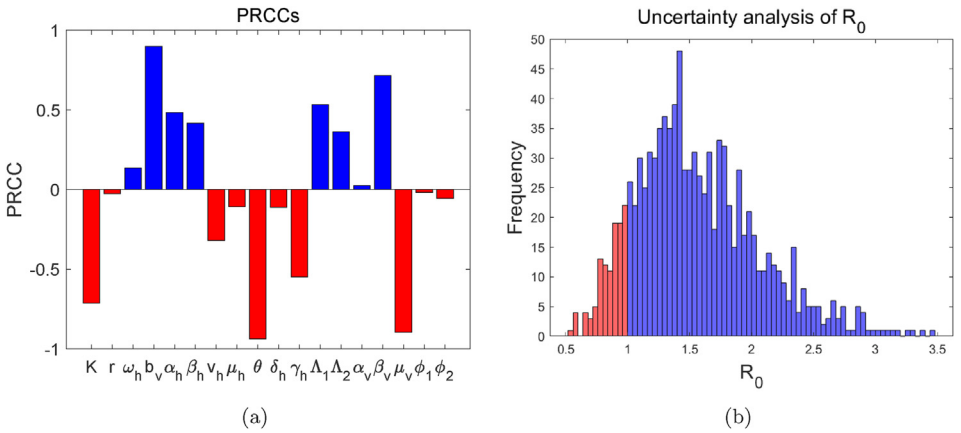

Fig. 2. Sensitivity analysis and uncertainty analysis of the basic reproduction number R_0. (a) shows the sensitivity indices of R_0, and (b) shows histogram obtained from LHS using a sample size of 1000 for R_0.

This indicates that persistent HLB bacterial infection is likely to occur. Furthermore, by numerical calculation, we obtain the mean and standard deviation of R_0 are 1.5611 and 0.4973, respectively.

We consider the influence of two model parameter γ_h and μ_v on the basic reproduction number R_0 in Fig. 3. We can observe from Fig. 3 that R_0 is very sensitive to γ_h and μ_v, it is seen that as γ_h and μ_v increase, the basic reproduction number R_0 decreases quickly.

The dynamics of the basic reproduction number of our model as a function of insecticide resistance intensities φ_1 and φ_2 is depicted in Fig. 4. It is seen that as the resistance coefficients φ_1 and φ_2 increase, the basic reproduction number R_0 decreases slowly. This indicates that the intensity of insecticide resistance present in ACP population may slightly reduce the effectiveness of control measures, which is in agreement with results of sensitivity analysis (see Fig. 2(a)).

In order to reduce the number of trees infected by HLB disease, two possible control measures have been considered in this paper, including removal of diseased trees and application of insecticides. The objective of this paper is to analyze the effect of three controls on the transmission of HLB, and explore the optimal solution of the optimality system (4.1) and the corresponding optimal control by using the forward-backward sweep method. The initial numbers of susceptible citrus trees and ACP are assumed that $S_h(0) = 500$, $V_h(0) = 492$, $S_{v1}(0) = 30000$, $S_{v2}(0) = 20000$. Then we assume that the initial numbers of

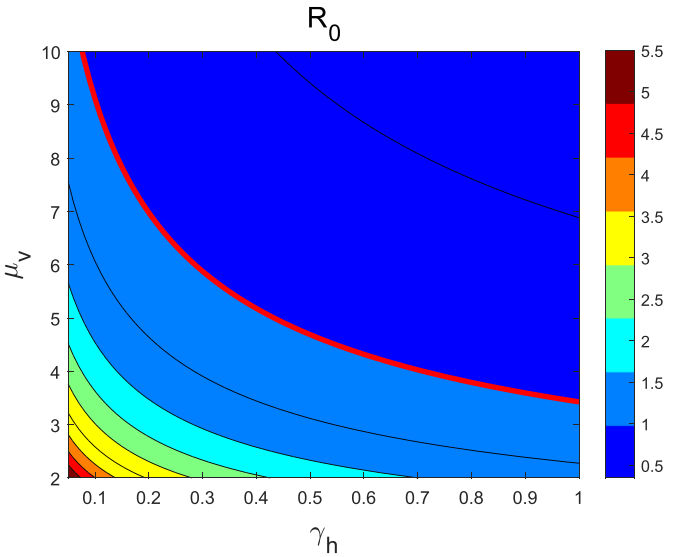

Fig. 3. The basic reproduction number of model (2.1) as a function of disease related death rate γ_h and natural mortality rate of ACP μ_v. The red curve indicates that the basic regeneration number R_0 is equal to one.

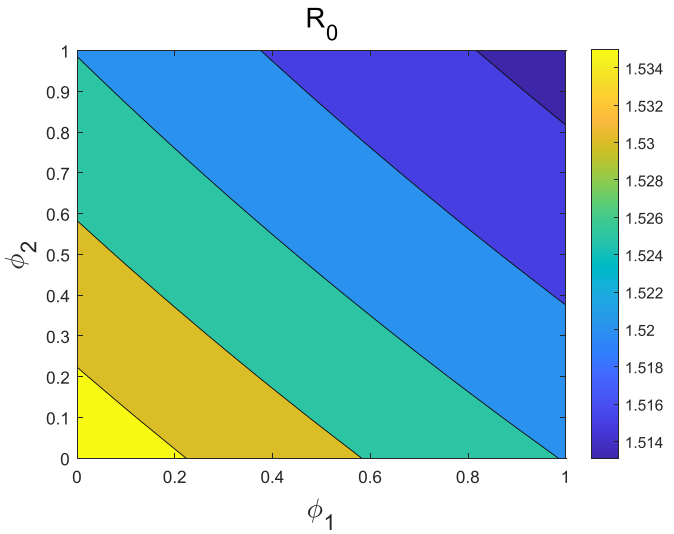

Fig. 4. The basic reproduction number of model (2.1) as a function of resistance intensities φ_1 and φ_2.

infectious citrus trees and ACP are $E_h(0) = 3$, $I_h(0) = 5$, $I_{v1}(0) = 20$, $I_{v2}(0) = 10$, respectively. In addition, the control intensity coefficients $\rho_1 = 10\mu_h$, $\rho_2 = 20\mu_v$ and $\rho_1 = 5\mu_v$. In the simulations, the values of other parameters are taken from Table 2.

In (Yan & Zou, 2008), the authors point out fixing the right weights in practical problems is a very difficult task which requires an amount of work on data analysis and fitting. For the weight factors in the objective function, we choose $A_1 = 1000$, $A_2 = 1000$, $A_3 = 0.01$, $A_4 = 100$ and $A_5 = 100$. Then the weights in the simulations here are only of theoretical sense to illustrate the control strategies proposed.

The following algorithm is used to compute the optimal controls and state values using a Runge-Kutta method of the fourth order. As illustrated in (Agusto & Khan, 2018), we should first give an initial estimate for the control quintuple, then solve the state variables forward in time by using the dynamics (4.1). The results obtained for the state variables are substituted into the adjoint equation (4.6). These adjoint equations with given final conditions (4.8) are then solved backward in time. Both the state and adjoint values are then used to update the control, and the process is repeated until the current state, adjoint, and controls values converge sufficiently.

The numbers of infectious citrus trees and infectious ACP under different control levels are depicted in Fig. 5. In view of reducing the total number of the diseased citrus trees (or the diseased ACP), we can observe that the optimal control strategy is consistent with the upper bound control strategy and is superior to the constant control. The enhancement of the level of

Table 3
The costs of the objective function under different weights and control measures.

[1 pt] $(A_1, A_2, A_3, A_4, A_5)$	$J(0, 0)$	$J(0.2, 0.2)$	$J(0.4, 0.4)$	$J_{max}(1, 1)$	$J_{opt}(u_h^*, u_v^*)$
(1000,1000,0.01,100,100)	10524	8064	7502	6716	6703
(800,1000,0.01,1000,1000)	10424	8077	7739	8484	7517
(1000,10000,0.01,10000,1000)	9191	7521	7203	7297	6955
(500,1000,0.01,500,600)	10248	7951	7512	7498	7076
(1000,2000,0.01,1000,2000)	19567	15589	14930	15694	14052

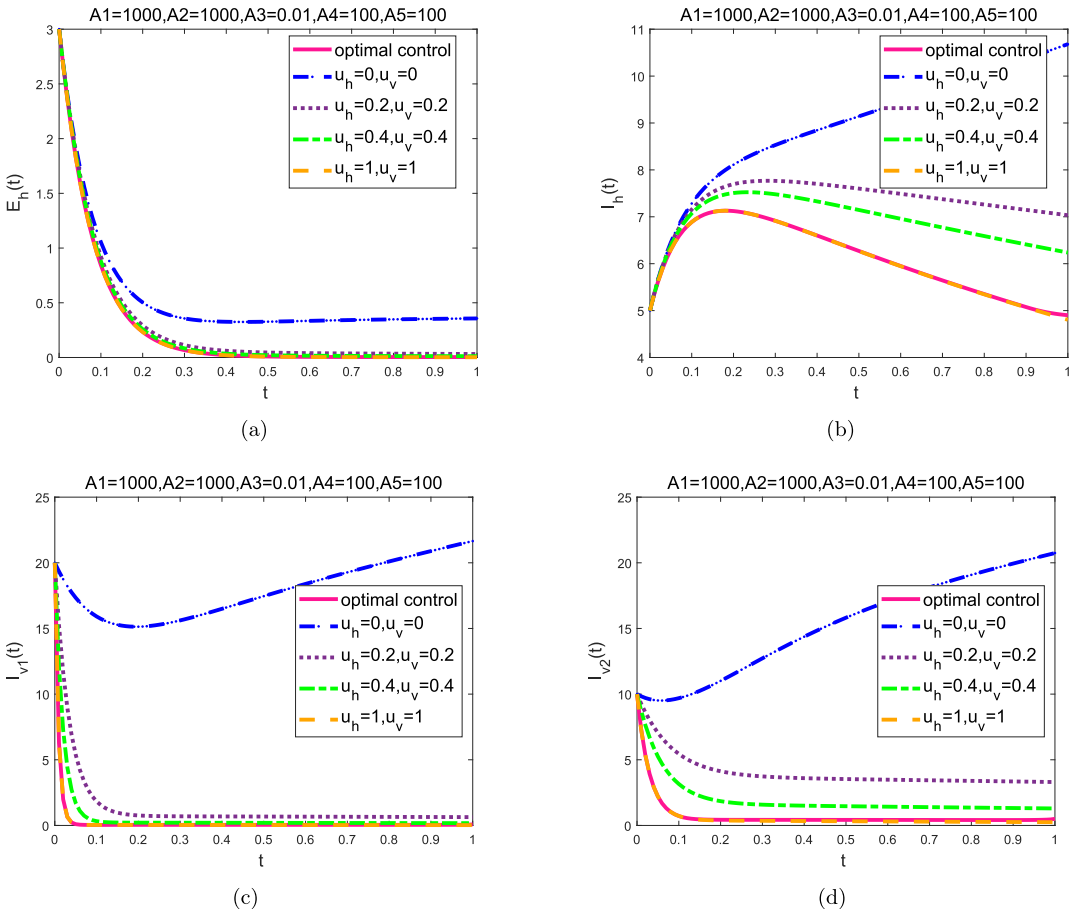

Fig. 5. Number of infectious citrus trees and infectious ACP under different control levels, (a) exposed citrus trees, (b) infected citrus trees, (c) infected sensitive ACP, (d) infected resistant ACP.

control can achieve significant effects on both the number of hosts and vectors. Moreover, it follows from Table 3 that the cost of the optimal control is less than that of the upper bound control. We may conclude that the optimal control strategy appears to offer a promising measure for HLB control.

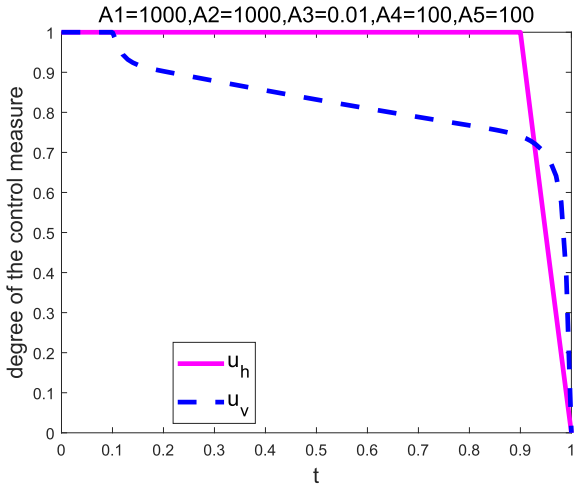

Fig. 6. Optimal control law of u_h and u_v.

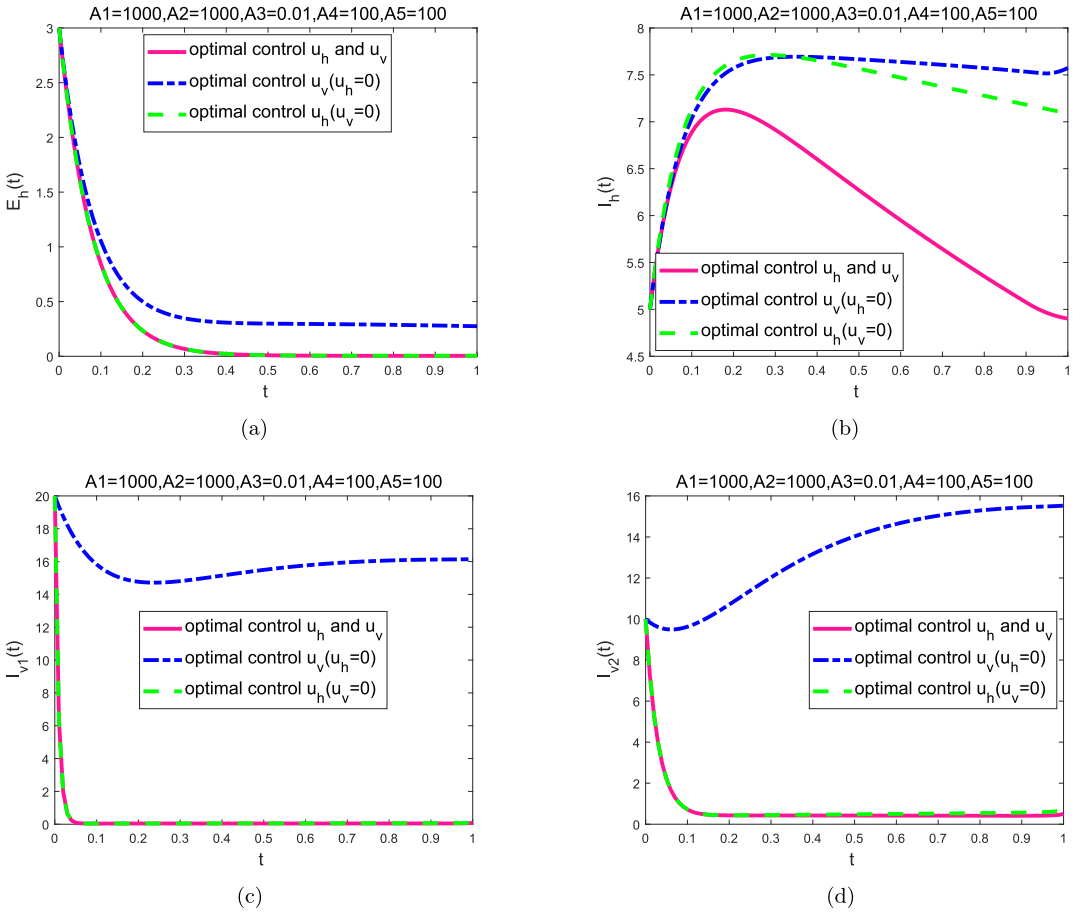

Fig. 7. Number of infectious citrus treess and infectious ACP under different optimal control measures, i.e. (I) u_h and u_v; (II) u_h, $(u_v = 0)$; (III)u_v, $(u_h = 0)$.

Fig. 6 gives the optimal control profile for u_h and u_v. It shows that, the control variable u_h starts at the upper bound 1 for about 90% time and then gradually decreases to the lower bound 0 at the end of the simulation period. While the control variables u_v start at the upper bound for a shorter time and slowly decrease to the lower bound at the end of the simulation period.

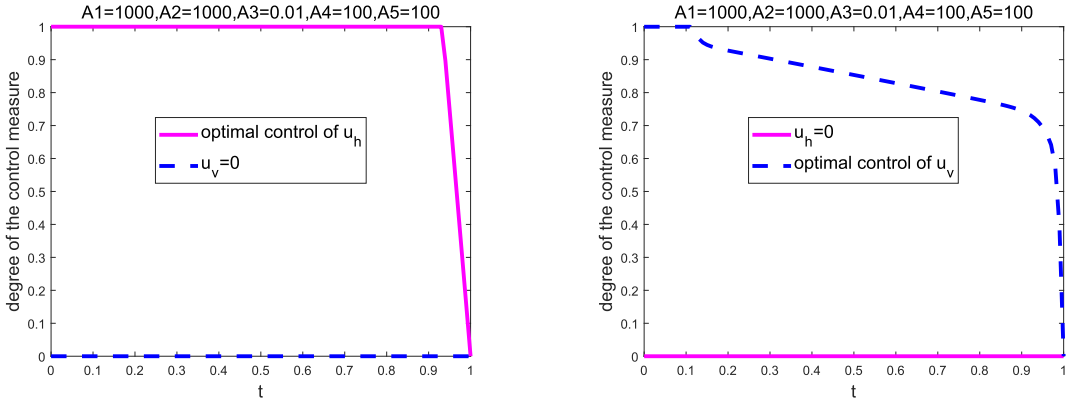

Fig. 8. Optimal control law of: (I) u_h, ($u_v = 0$); (II) u_v, ($u_h = 0$).

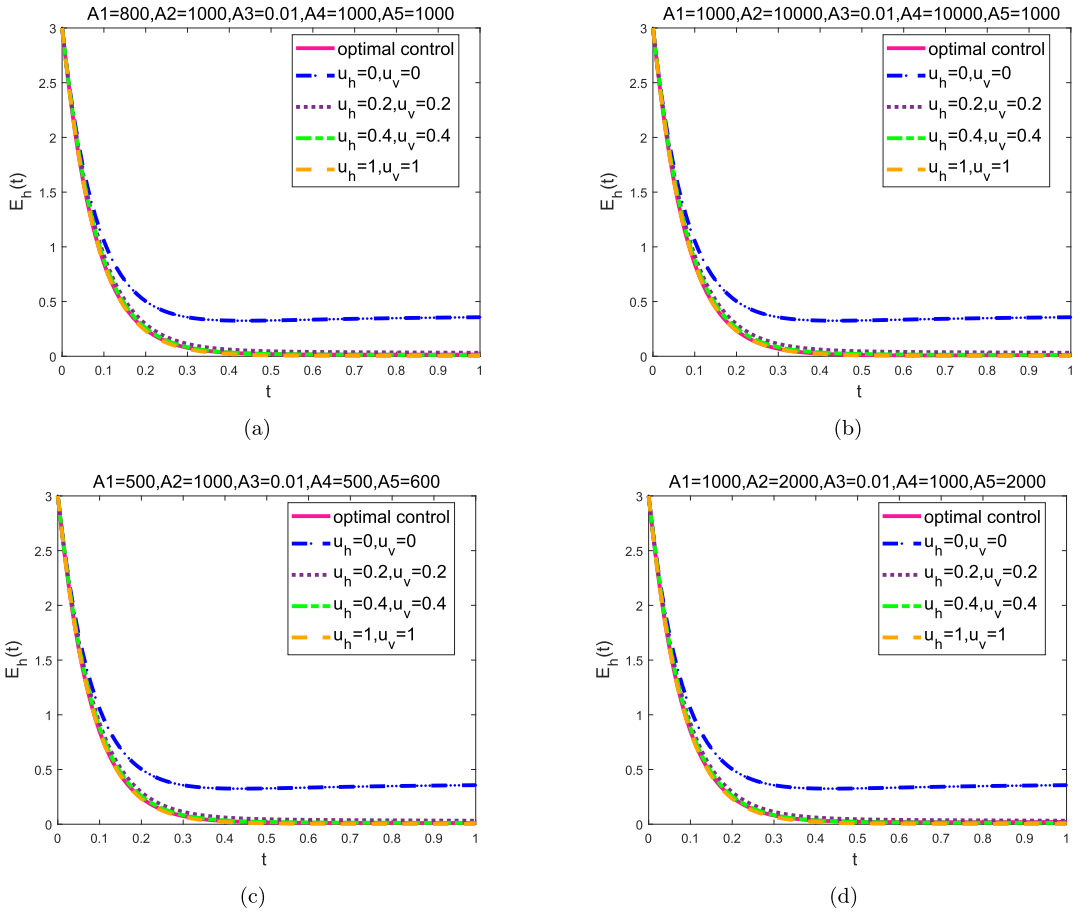

Fig. 9. Comparison of the number of exposed citrus treess $E_h(t)$ with different weights.

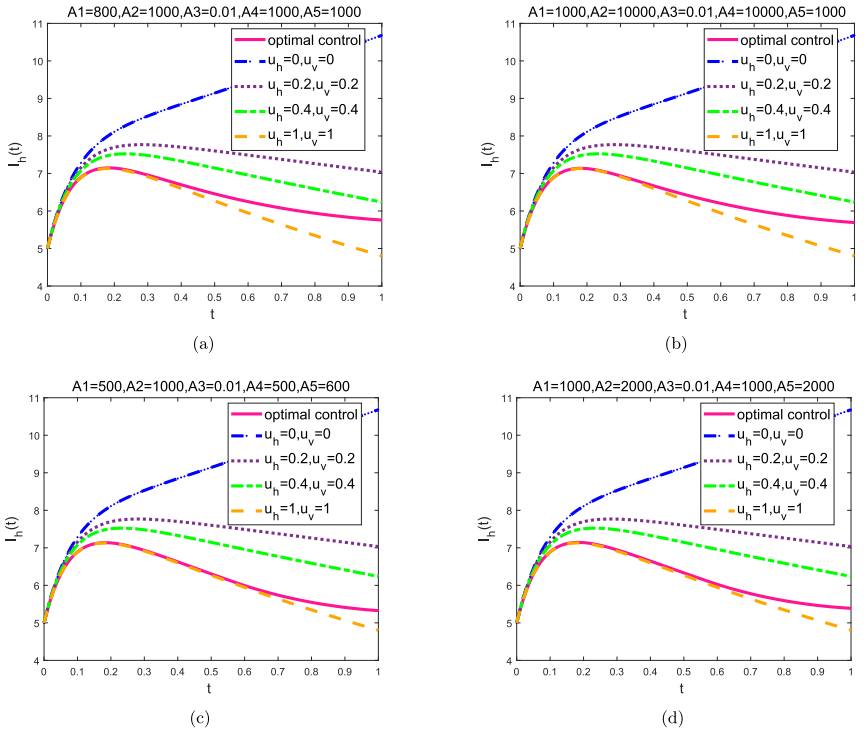

Fig. 10. Comparison of the number of infectious citrus treess $I_h(t)$ with different weights.

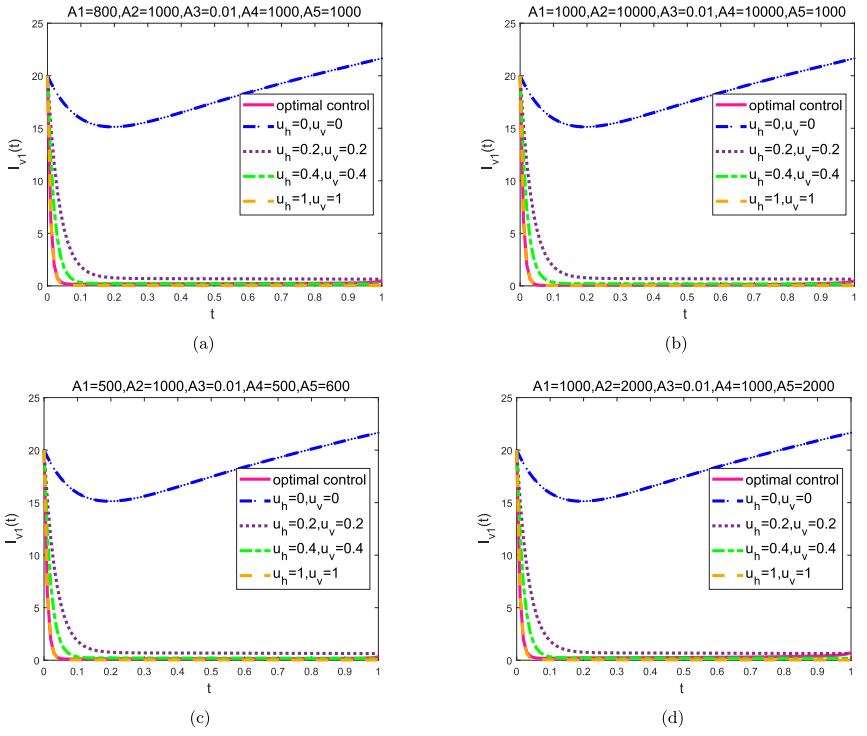

Fig. 11. Comparison of the number of infected sensitive ACP $I_{v1}(t)$ with different weights.

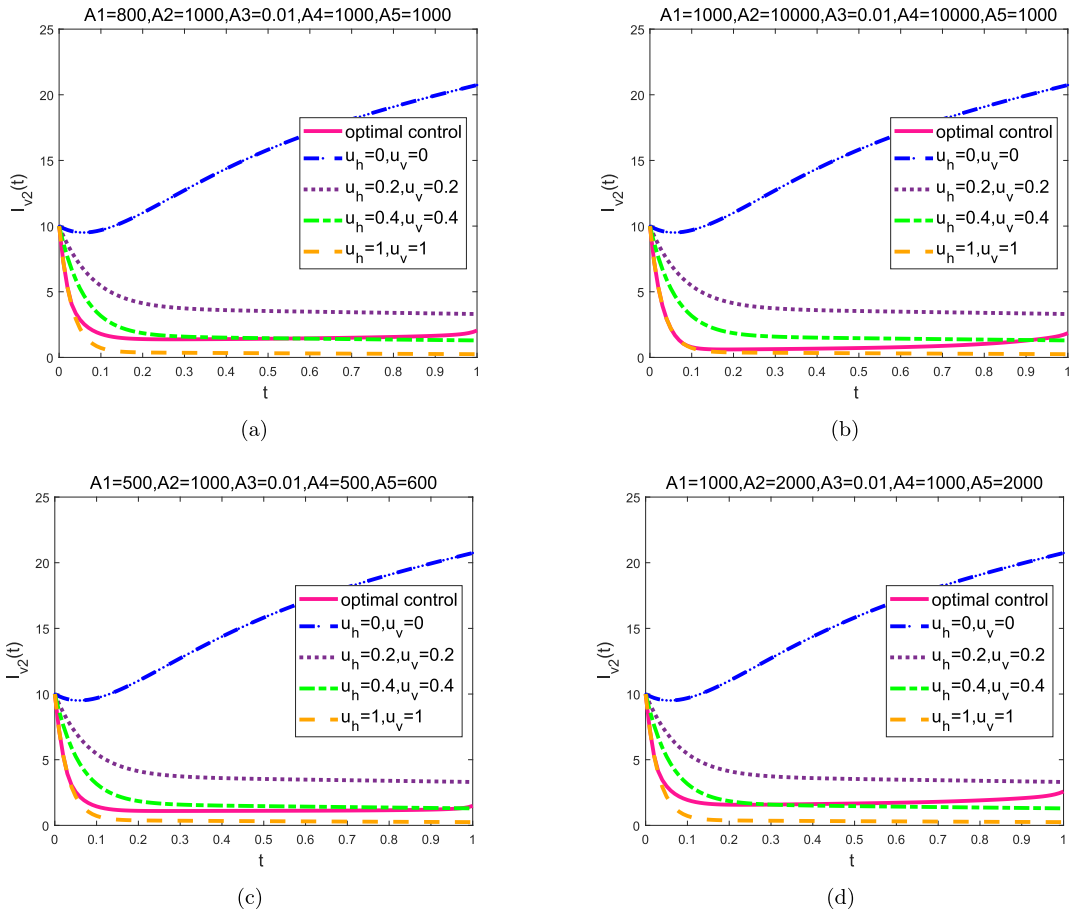

Fig. 12. Comparison of the number of infected resistant ACP $I_{v2}(t)$ with different weights.

Fig. 7 presents the number of infectious citrus trees and infectious ACP under different control strategies. These control strategies are: (I) u_h and u_v; (II) u_h, ($u_v = 0$); (III) u_v, ($u_h = 0$). From Fig. 7, we can observe that: (1) the cost of implementing strategy (II) is lower than that of implementing strategy (III); (2) the number of infectious citrus trees is the smallest when implementing strategy (I), while the number of infectious citrus trees is the largest when implementing strategy (II); (3) in addition to strategy (I), the final number of diseased ACP is the least when applying strategy (III), and the final number of diseased ACP is the most when applying strategy (II). These results imply that multiple control strategies should be adopted simultaneously to control the spread of HLB.

The optimal control trajectories under different control measures are presented in Fig. 8. It can be seen that in the early phase of HLB outbreak, the upper bound control strategies should be adopted in most cases to suppress the transmission of the disease.

Figs. 9–13 show the trajectories of the infectious citrus trees, the infectious ACP, and the optimal controls with different weights in objective function, respectively. Based on the simulation results, we can see that the weights have a great impact on the control cost (see Table 3), but have little or no effect on the spread of HLB. Consequently, the weights in the objective function have little impact on the optimal control strategy (Fig. 13).

6. Conclusion

In this paper, a deterministic mathematical model was first used to formulate the transmission dynamics of HLB between the ACP and the citrus tress, which incorporated the insecticide resistance of ACP. The stability of equilibria of the model was analyzed using the basic reproduction number R_0, derived by the next generation matrix. Theoretical results have shown that the disease free equilibrium is locally asymptotically stable if $R_0 < 1$, whereas the HLB system (2.1) is persistent if $R_0 > 1$.

Furthermore, we used the optimization theory and the three time-dependent control variables to establish an optimal control strategy for exclusion of HLB infection by minimizing the number of exposed and infected trees. The necessary conditions for the existence of optimal solution of control problem are obtained by using Pontryagin's Maximum Principle.

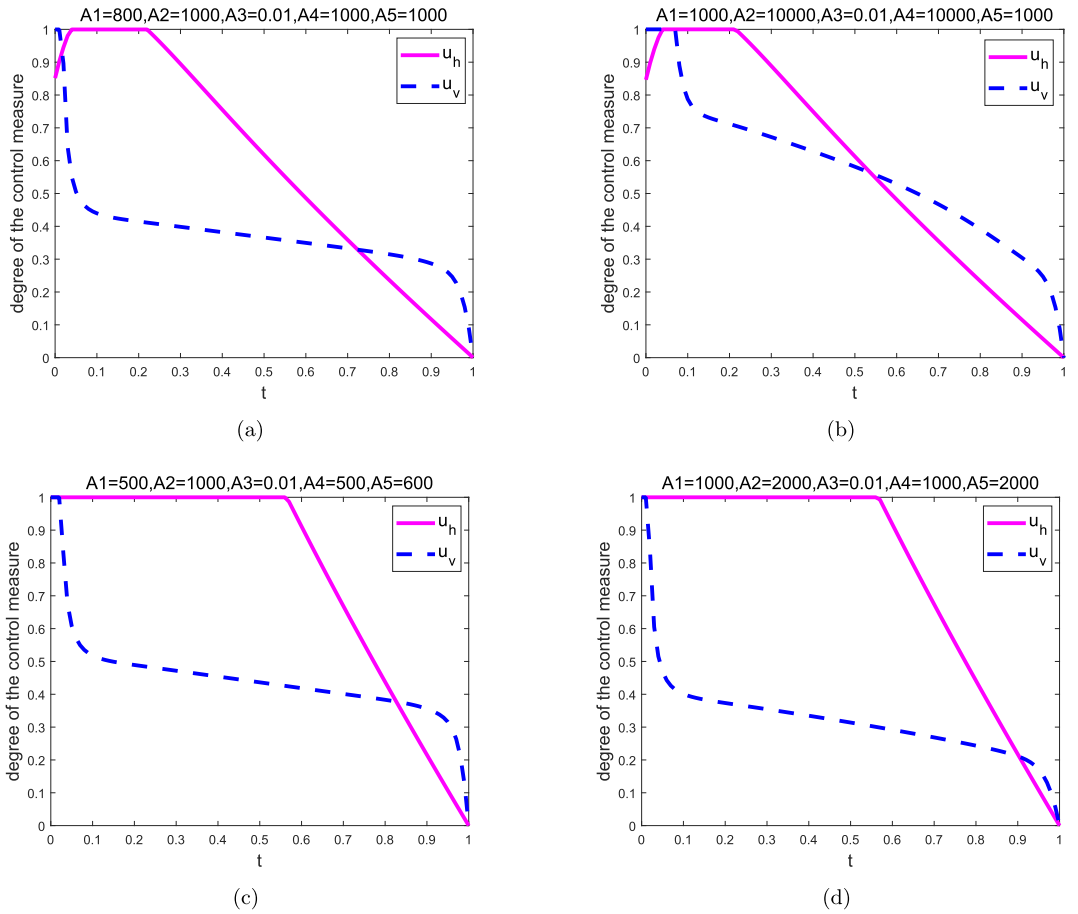

Fig. 13. Optimal control law of u_h and u_v with different weights.

Finally, we verified the analytical results by numerical simulations. Based on analytical and the numerical simulation results, the main conclusions of this paper can be summarized as follows:

(1) The intensity of insecticide resistance present in ACP population may slightly reduce the effectiveness of control measures.
(2) The optimal control strategy is superior to the constant control strategy in decreasing the prevalence of the infected citrus trees, and the cost of implementing optimal control is much lower than that of the constant control strategy.
(3) In the early phase of the transmission of HLB, spraying insecticides to kill ACP is more effective than other control strategies in reducing the number of the infected ACP.
(4) The weights in the objective function have little impact on the optimal control strategy.

Data availability

All data generated or analyzed during this study are included in this article.

Declaration of competing interest

The authors declare that they have no conflicts of interest regarding the publication of this paper.

Acknowledgements

The research has been supported by the Natural Science Foundation of China (11961003, 11901110), The Natural Science Foundation of Jiangxi Province (20192ACBL20004), and The Science and Technology Project of Education Department of Jiangxi Province (GJJ190740, GJJ201406).

Appendix A. The proof of global asymptotical stability of positive equilibrium $(\tilde{S}_h^0, \tilde{V}_h^0)$

Denote $\tilde{N}_h = \tilde{S}_h + \tilde{V}_h$, then system (3.7) is equivalent to the following system

$$\begin{cases} \dfrac{d\tilde{N}_h}{dt} = r(K - 2\zeta_2) - (r + \mu_h + \tilde{\eta}_h)\tilde{N}_h + \theta\tilde{\eta}_h\tilde{V}_h, \\ \dfrac{d\tilde{V}_h}{dt} = \nu_h\tilde{N}_h - \nu_h\tilde{V}_h - (1-\theta)\tilde{\eta}_h\tilde{V}_h - d_2\tilde{V}_h. \end{cases} \tag{6.1}$$

Denote $x = \tilde{N}_h$, $y = \tilde{V}_h$, $c_0 = r(K - 2\zeta_2)$, $c_1 = r + \mu_h + \tilde{\eta}_h$, $c_2 = \theta\tilde{\eta}_h$, $c_3 = \nu_h$ and $c_4 = \nu_h + (1-\theta)\tilde{\eta}_h + d_2$. By calculating, $c_1c_4 - c_2c_3 = (r + \mu_h)(\nu_h + (1-\theta)\tilde{\eta}_h + d_2) + \tilde{\eta}_h((1-\theta)\tilde{\eta}_h + d_2) + (1-\theta)\tilde{\eta}_h\nu_h > 0$. So system (6.1) is given by

$$\begin{cases} \dfrac{dx}{dt} = c_0 - c_1x + c_2y, \\ \dfrac{dy}{dt} = c_3x - c_4y. \end{cases} \tag{6.2}$$

It is easy to obtain, the model (6.2) has a unique positive equilibrium point (x^*, y^*), where

$$x^* = \frac{c_0c_4}{c_1c_4 - c_2c_3},$$
$$y^* = \frac{c_0c_3}{c_1c_4 - c_2c_3}.$$

Thus system (6.2) can be rewritten as

$$\begin{cases} \dfrac{dx}{dt} = -c_1(x - x^*) + c_2(y - y^*), \\ \dfrac{dy}{dt} = c_3(x - x^*) - c_4(y - y^*). \end{cases} \tag{6.3}$$

We define a Lyapunov function

$$L(x, y) = \frac{(x - x^*)^2}{2} + \frac{c_2}{c_3}\frac{(y - y^*)^2}{2}.$$

Then the derivative of function $L(x, y)$ along solutions of system (6.3) is given by

$$\begin{aligned} \frac{dL}{dt} &= (x - x^*)[-c_1(x - x^*) + c_2(y - y^*)] + \frac{c_2}{c_3}(y - y^*)[c_3(x - x^*) - c_4(y - y^*)] \\ &= -c_1(x - x^*)^2 + 2c_2(x - x^*)(y - y^*) - \frac{c_2c_4}{c_3}(y - y^*)^2 \\ &= -c_1\left[(x - x^*) - \frac{c_2}{c_1}(y - y^*)\right]^2 - \frac{c_2}{c_1c_3}(c_1c_4 - c_2c_3)(y - y^*)^2. \end{aligned}$$

Thus, we have $\frac{dL}{dt} \le 0$ and the equality holds if and only if $x = x^*$ and $y = y^*$, that is, $\tilde{S}_h = \tilde{S}_h^0$ and $\tilde{V}_h = \tilde{V}_h^0$. It follows that the unique positive equilibrium point $(\tilde{S}_h^0, \tilde{V}_h^0)$ of (3.12) is globally asymptotically stable.

References

Agusto, F. (2013). Optimal isolation control strategies and cost-effectiveness analysis of a two-strain avian influenza model. *Biosystems, 113*, 155–164.
Agusto, F., & Khan, M. (2018). Optimal control strategies for dengue transmission in Pakistan. *Mathematical Biosciences, 305*, 102–121.

Agusto, F., & Lenhart, S. (2013). Optimal control of the spread of malaria superinfectivity. *Journal of Biological Systems, 21*, 1–26.
Alzahrani, E. O., Ahmad, W., Khan, M. A., & Malebary, S. J. (2021). Optimal control strategies of zika virus model with mutant. *Communications in Nonlinear Science and Numerical Simulation, 93*, 105532.
Arredondo Valdés, R., Delgado Ortiz, J. C., Beltrán Beache, M., Anguiano Cabello, J., Cerna Chávez, E., Rodríguez Pagaza, Y., & Ochoa Fuentes, Y. M. (2016). A review of techniques for detecting Huanglongbing (greening) in citrus. *Canadian Journal of Microbiology, 62*, 803–811.
Blower, S. M., & Dowlatabadi, H. (1994). Sensitivity and uncertainty analysis of complex models of disease transmission: An hiv model, as an example. *International Statistical Review/Revue Internationale de Statistique*, 229–243.
Bovè, J. M. (2006). Huanglongbing: A destructive, newly-emerging, century-old disease of citrus. *Journal of Plant Pathology, 88*, 7–37.
Chiyaka, C., Singer, B. H., Halbert, S. E., Morris, J. G., & van Bruggen, A. H. (2012). Modeling Huanglongbing transmission within a citrus tree. *Proceedings of the National Academy of Sciences, 109*, 12213–12218.
Chowdhury, J., Al Basir, F., Takeuchi, Y., Ghosh, M., & Roy, P. K. (2019). A mathematical model for pest management in jatropha curcas with integrated pesticides-an optimal control approach. *Ecological Complexity, 37*, 24–31.
Fleming, W. H., & Rishel, R. W. (2012). *Deterministic and stochastic optimal control* (Vol. 1). Springer Science & Business Media.
Gao, S., Luo, L., Yan, S., Meng, X., et al. (2018). Dynamical behavior of a novel impulsive switching model for HLB with seasonal fluctuations. *Complexity*, 1–11, 2018.
Gottwald, T. R. (2010). Current epidemiological understanding of citrus Huanglongbing. *Annual Review of Phytopathology, 48*, 119–139.
Hu, J., Jiang, J., & Wang, N. (2018). Control of citrus huanglongbing via trunk injection of plant defense activators and antibiotics. *Phytopathology, 108*, 186–195.
Jackson, M., & Chen-Charpentier, B. M. (2019). Modeling plant virus propagation with seasonality. *Journal of Computational and Applied Mathematics, 345*, 310–319.
Jacobsen, K., Stupiansky, J., & Pilyugin, S. S. (2013). Mathematical modeling of citrus groves infected by Huanglongbing. *Mathematical Biosciences and Engineering, 10*, 705–728.
Jeger, M., Madden, L., & Van Den Bosch, F. (2018). Plant virus epidemiology: Applications and prospects for mathematical modeling and analysis to improve understanding and disease control. *Plant Disease, 102*, 837–854.
Khan, M. A., Fatmawatic, et al. (2021). Dengue infection modeling and its optimal control analysis in east java, Indonesia. *Heliyon, 7*, Article e06023.
Khan, M. F., Alrabaiah, H., Ullah, S., Khan, M. A., Farooq, M., bin Mamat, M., & Asjad, M. I. (2021). A new fractional model for vector-host disease with saturated treatment function via singular and non-singular operators. *Alexandria Eng. J., 60*, 629–645.
Lee, J. A., Halbert, S. E., Dawson, W. O., Robertson, C. J., Keesling, J. E., & Singer, B. H. (2015). Asymptomatic spread of Huanglongbing and implications for disease control. *Proceedings of the National Academy of Sciences, 112*, 7605–7610.
Lenhart, S., & Workman, J. T. (2007). *Optimal control applied to biological models*. CRC press.
Li, W., Ji, J., Huang, L., & Wang, J. (2020). Bifurcations and dynamics of a plant disease system under non-smooth control strategy. *Nonlinear Dynamics*, 1–21.
Li, J., Trivedi, P., & Wang, N. (2015). Field evaluation of plant defense inducers for the control of citrus Huanglongbing. *Phytopathology, 106*, 37–46.
McCollum, G., & Baldwin, E. (2017). Huanglongbing: Devastating disease of citrus. *Horticultural Reviews, 44*, 315–361.
Meng, X., & Li, Z. (2010). The dynamics of plant disease models with continuous and impulsive cultural control strategies. *Journal of Theoretical Biology, 266*, 29–40.
Mingxue, D. (2009). Forming process and basis and technological points of the theory emphasis on control citrus psylla for integrated control Huanglongbing. *Chin. Agric. Sci. Bull., 25*, 358–363.
Okosun, K. O., Rachid, O., & Marcus, N. (2013). Optimal control strategies and cost-effectiveness analysis of a malaria model. *Biosystems, 111*, 83–101.
Pei, Y., Chen, M., Liang, X., Xia, Z., Lv, Y., & Li, C. (2016). Optimal control problem in an epidemic disease sis model with stages and delays. *International Journal of Biomathematics, 9*, 1–22.
Pontryagin, L. S. (2018). *Mathematical theory of optimal processes*. Routledge.
Taylor, R. A., Mordecai, E. A., Gilligan, C. A., Rohr, J. R., & Johnson, L. R. (2016). Mathematical models are a powerful method to understand and control the spread of Huanglongbing. *PeerJ, 4*, 2642–2660.
Tu, Y., Gao, S., Liu, Y., Chen, D., & Xu, Y. (2019). Transmission dynamics and optimal control of stage structured HLB model. *Mathematical Biosciences and Engineering, 16*, 5180–5205.
R. G. d. Vilamiu, S. Ternes, G. A. Braga, F. F. Laranjeira, A model for Huanglongbing spread between citrus plants including delay times and human intervention, in: AIP conference proceedings, volume Vol. 1479, American Institute of Physics, pp. 2315-2319.
Wang, N., & Trivedi, P. (2013). Citrus huanglongbing: A newly relevant disease presents unprecedented challenges. *Phytopathology, 103*, 652–665.
Yan, X., & Zou, Y. (2008). Optimal and sub-optimal quarantine and isolation control in sars epidemics. *Mathematical and Computer Modelling, 47*, 235–245.
Zhang, H., & Georgescu, P. (2015). The influence of the multiplicity of infection upon the dynamics of a crop-pest-pathogen model with defence mechanisms. *Applied Mathematical Modelling, 39*, 2416–2435.
Zhang, F., Qiu, Z., Huang, A., & Zhao, X. (2021). Optimal control and cost-effectiveness analysis of a Huanglongbing model with comprehensive interventions. *Applied Mathematical Modelling, 90*, 719–741.
Zhang, F., Qiu, Z., Zhong, B., Feng, T., & Huang, A. (2020). Modeling citrus Huanglongbing transmission within an orchard and its optimal control. *Mathematical Biosciences and Engineering, 17*, 2048–2069.
Zhao, X.-Q. (2003). *Dynamical systems in population biology* (Vol. 16). Springer.
Zhao, W., Li, J., Zhang, T., Meng, X., & Zhang, T. (2017). Persistence and ergodicity of plant disease model with markov conversion and impulsive toxicant input. *Communications in Nonlinear Science and Numerical Simulation, 48*, 70–84.